EPJ manuscript No.
(will be inserted by the editor)

Inhomogeneous Tsallis distributions in the HMF model

P.H Chavanis and A. Campa

[1] Laboratoire de Physique Théorique (IRSAMC), CNRS and UPS, Université de Toulouse, F-31062 Toulouse, France
[2] Complex Systems and Theoretical Physics Unit, Health and Technology Department, Istituto Superiore di Sanità, and INFN Roma 1, Gruppo Collegato Sanita, 00161 Roma, Italy

To be included later

Abstract. We study the maximization of the Tsallis functional at fixed mass and energy in the HMF model. We give a thermodynamical and a dynamical interpretation of this variational principle. This leads to q-distributions known as stellar polytropes in astrophysics. We study phase transitions between spatially homogeneous and spatially inhomogeneous equilibrium states. We show that there exists a particular index $q_c = 3$ playing the role of a canonical tricritical point separating first and second order phase transitions in the canonical ensemble and marking the occurence of a negative specific heat region in the microcanonical ensemble. We apply our results to the situation considered by Antoni & Ruffo [Phys. Rev. E **52**, 2361 (1995)] and show that the anomaly displayed on their caloric curve can be explained naturally by assuming that, in this region, the QSSs are polytropes with critical index $q_c = 3$. We qualitatively justify the occurrence of polytropic (Tsallis) distributions with compact support in terms of incomplete relaxation and inefficient mixing (non-ergodicity). Our paper provides an exhaustive study of polytropic distributions in the HMF model and the first plausible explanation of the surprising result observed numerically by Antoni & Ruffo (1995). In the course of our analysis, we also report an interesting situation where the caloric curve presents both microcanonical first and second order phase transitions.

PACS. 0 5.20.-y Classical statistical mechanics - 05.45.-a Nonlinear dynamics and chaos - 05.20.Dd Kinetic theory - 64.60.De Statistical mechanics of model systems

1 Introduction

Systems with long-range interactions are numerous in nature. Some examples include self-gravitating systems (galaxies), two-dimensional turbulence (vortices), chemotaxis of bacterial populations (clusters) and some models in plasma physics [1]. These systems are fascinating because they present striking features that are absent in systems with short-range interactions such as negative specific heats in the microcanonical ensemble, numerous types of phase transitions, ensembles inequivalence, unusual thermodynamic limit, violent collisionless relaxation, long-lived quasi stationary states (QSS), non-Boltzmannian distributions, out-of-equilibrium phase transitions, re-entrant phases, non-ergodic behavior, slow collisional relaxation, dynamical phase transitions, algebraic decay of the correlation functions... We refer to [2,3] for some recent reviews on the subject.

In order to understand these strange properties in a simple setting, a toy model of systems with long-range interactions has been actively studied. It consists of N particles moving on a ring and interacting via a cosine potential. This model has been introduced by many authors [4-8] at about the same period with different motivations (see a short history in [9]). Let us mention for example that Pichon [7] introduced this model to explain the formation of bars in disk galaxies, giving it a physical application. This model is now known as the Hamiltonian Mean Field (HMF) model. This abbreviation was coined by Antoni & Ruffo [8] and it stood at that time either for Hamiltonian or Heisenberg Mean Field model since the HMF model can be viewed as a mean field XY model with long-range interactions (i.e. not restricted to the nearest neighbors). In fact, this model was first introduced much earlier (this is not well-known) by Messer & Spohn [10] and called the cosine model[1]. They rigorously studied phase transitions in the canonical ensemble by evaluating the free energy and exhibited a second order phase transition between a homogeneous phase and a clustered phase below a critical temperature $T_c = 1/2$.

In their seminal paper, Antoni & Ruffo [8] studied the statistical mechanics of this model in the canonical ensemble (CE) directly from the partition function and performed N-body simulations in the microcanonical ensemble (MCE). They started from a waterbag[2] initial condi-

[1] These authors mention that this "cosine model" was suggested by G. Battle [11].

[2] A waterbag distribution corresponds to a uniform distribution function $f(\theta, v) = f_0$ in the domain $[-\theta_m, \theta_m] \times [-v_m, v_m]$ surrounded by "vaccum" $f(\theta, v) = 0$. It can have different magnetization $0 \leq M_0 \leq 1$.

tion with magnetization $M_0 \equiv M(0) = 1$ and plotted in their Fig. 4 the caloric curve giving the averaged kinetic temperature $T = 2E_{kin}/N$ as a function of the energy U. They compared their numerical curve with the Boltzmann prediction of statistical equilibrium in the canonical ensemble. They found a good agreement at high and low energies. However, close to the critical energy $U_c = 3/4$ (corresponding to $T_c = 1/2$), the results differ from the canonical prediction. In particular, the system bifurcates from the homogeneous branch at a smaller energy $U \sim 0.6-0.7$ and the caloric curve $T(U)$ displays a region of negative specific heats. Antoni & Ruffo [8] interpreted this result either as (i) a nonequilibrium effect, or (ii) as a manifestation of ensembles inequivalence due to the non-additivity of the energy. However, it is clear from the previous work of Inagaki [6] and the application of the Poincaré theorem that the ensembles are equivalent for the HMF model (as confirmed later by various methods [12,9,2]). Therefore, this negative specific heats region is not a manifestation of ensembles inequivalence but rather a nonequilibrium effect.

Latora *et al.* [13,14] again performed microcanonical simulations of the HMF model. They confirmed the "anomaly" (negative specific heats region) reported by Antoni & Ruffo [8] and observed many other anomalies in that region such as non-Gaussian distributions, anomalous diffusion, Lévy walks and dynamical correlations in phase-space. Furthermore, they showed that the thermodynamic limit $N \to +\infty$ and the infinite time limit $t \to +\infty$ do not commute. They evidenced two regimes in the dynamics. On a short timescale, of the order of the dynamical time $t_D \sim 1$, the system reaches a quasistationary state (QSS). Then, on a much longer timescale $t_{relax}(N)$, the system relaxes towards the Boltzmann distribution of statistical equilibrium. They showed that the relaxation time increases rapidly (algebraically) with the number of particles N so that, at the thermodynamic limit $N \to +\infty$, the system remains permanently in the QSS. It is thus clear from this study that the different anomalies mentioned above characterize the QSS, not the statistical equilibrium state that is reached much later. In particular, the results of Antoni & Ruffo [8] and Latora *et al.* [14] show that the QSS is non-Boltzmannian in the region close to the critical energy U_c. Latora *et al.* [14] thus proposed to describe the QSS in terms of Tsallis [15] generalized thermodynamics leading to q-distributions. Note that there is no reason why the QSS should be Boltzmannian (in the usual sense) since it is an out-of-equilibrium structure. Therefore, the comparison of the numerical caloric curve with the Boltzmann equilibrium caloric curve $T(U)$ is not justified *a priori*.

After the conference in Les Houches in 2002, and inspired by the results in astrophysics and 2D turbulence presented by one of the authors [16], several groups of researchers [17,9,18,19] started to interpret the QSSs observed in the HMF model in terms of Lynden-Bell's [20] statistical theory of violent relaxation based on the Vlasov equation. This is a fully predictive theory based on *standard thermodynamics* but taking into account the specificities of the Vlasov equation (Casimir constraints). Applying the Lynden-Bell theory to the HMF model (for waterbag initial conditions), an out-of-equilibrium phase transition was discovered in [18,19]. For a given value of the energy U, there exists a critical value of the initial magnetization $(M_0)_{crit}(U)$ such that: for $M_0 < (M_0)_{crit}(U)$ the stable Lynden-Bell distribution (i.e. most probable state) is homogeneous (non-magnetized) and for $M_0 > (M_0)_{crit}(U)$ the stable Lynden-Bell distribution is inhomogeneous (magnetized). For $U = 0.69$, the critical magnetization is $(M_0)_{crit} = 0.897$ [18,19]. More generally, there exists a critical line $(M_0)_{crit}(U)$ in the phase diagram separating homogeneous and inhomogeneous Lynden-Bell distributions. It was found later [21,22] that the system displays first and second order phase transitions separated by a tricritical point. There is also an interesting phenomenon of phase reentrance in the (f_0, U) plane predicted in [18] and numerically confirmed in [23]. Coming back to the specific value $U = 0.69$, direct numerical simulations of the HMF model for $M_0 < (M_0)_{crit}$ have shown that the Lynden-Bell prediction works fairly well [19]. This agreement is remarkable since there is no fitting parameter in the theory. This led the authors of [19] to argue that "Lynden-Bell's theory explains quasistationary states in the HMF model". A controversy started when some of these authors [17,24,2] concluded that "the approach of Tsallis is unsuccessful to explain QSSs".

However, caution was made by one author [25,18,26] who argued that the Lynden-Bell theory does not explain everything. Indeed, for initial magnetization $M_0 = 1$, the system is in the non-degenerate limit so that the Lynden-Bell entropy reduces to the Boltzmann entropy (with a different interpretation). Therefore, in this limit case, the Lynden-Bell theory leads exactly to the same prediction as the usual Boltzmann statistical theory but, of course, for a completely different reason. This observation led to a re-interpretation [26] of the caloric curve $T(U)$ obtained by Antoni & Ruffo [8] and Latora *al.* [14]. In this curve, the theoretical line should not be interpreted as the Boltzmann statistical equilibrium state but as the Lynden-Bell statistical equilibrium state[3]. They turn out to coincide in the case $M_0 = 1$ but this is essentially coincidental. With this new interpretation [26], the comparison reveals that the Lynden-Bell theory works well for large and low energies but that it fails for energies close to the critical energy. Therefore, *the Lynden-Bell theory does not explain the observations in the range* $[0.5, U_c]$. Chavanis [26] interpreted this disagreement as a result of *incomplete relaxation*. Indeed, it was emphasized by Lynden-Bell [20] himself that his approach implicitly assumes that the system "mixes efficiently" so that the ergodicity hypothesis which sustains his statistical theory applies. However, it has been observed in many cases of violent relaxation that the system does not mix efficiently so that the Lynden-Bell pre-

[3] As mentioned above, there is no reason to compare the QSS with the Boltzmann prediction that corresponds to the collisional regime reached for $t \to +\infty$. By contrast, it is fully relevant to compare the observed QSS with the Lynden-Bell prediction that applies to the collisionless regime.

diction fails (see various examples quoted in [25,26]). The qualitative reason is easy to understand [26]. Since violent relaxation is a purely inertial process (no collision), mixing is due to the fluctuations of the mean field potential caused by the fluctuations of the distribution function itself [20]. However, as the system approaches metaequilibrium (QSS), the fluctuations of the distribution function are less and less efficient (by definition!) and the system can be trapped in a QSS (a steady solution of the Vlasov equation on the coarse-grained scale) that is not the most mixed state. This is what happens in astrophysics (elliptical galaxies are *not* described by Lynden-Bell's distribution that has infinite mass [27]) and in certain situations of 2D turbulence [28-30]. The results of Antoni & Ruffo [8] and Latora *et al.* [14] reveal that the same phenomenon occurs for the HMF model close to the critical energy[4]. This is also visible on Fig. 8 of Bachelard *et al.* [31]. There is a huge region in the top right of the phase diagram where the Lynden-Bell theory does not work. This concerns in particular the point $U = 0.69$ and $M_0 = 1$, as anticipated in [18,26]. It is precisely this "no-man's land" region that Tsallis and coworkers have investigated [3]. In this region, standard statistical mechanics (i.e. Lynden-Bell's theory) does not seem to directly apply[5].

In their early work, Latora *et al.* [14] tried to fit the QSS by a q-distribution. They considered a distribution with $q = -5 < 1$ (in our notations) leading to power-law tails and introduced by hand an additional cut-off to make the distribution normalizable. This procedure is very *ad hoc*. Furthermore, even if we accept it, we can argue that it does not provide an impressive fit of the QSS. Recently, Campa *et al.* [34] have performed new simulations for initial magnetizations $M_0 = 0$ and $M_0 = 1$ and found that the QSS is very well-fitted by a semi-ellipse[6]. Similar results were obtained earlier by Yamaguchi *et al.* [17] for the $M_0 = 0$ case. They claimed that the QSS is not a q-distribution since it does not have power-law tails. However, Chavanis [26] remarked that a semi-ellipse is a q-distribution with $q = 3$! Since $q > 1$, this distribution has a compact support. Therefore, the numerical results of Campa *et al.* [34] and Yamaguchi *et al.* [17] show that the system tends to select a particular Tsallis distribution as a QSS[7]. Furthermore, the index $q = 3$ seems to play a particular role since Campa *et al.* [34] obtained the same index $q = 3$ in different situations (see their Fig. 4). However, until now, the reason for this particular value remains unknown. The fact that the QSS has a compact support is relatively natural in the phenomenology of incomplete violent relaxation. Indeed, when mixing is not very efficient, we expect that the high energy states are not sampled by the system. This leads to a confinement of the distribution which is a virtue of the Tsallis distributions with $q > 1$. A similar confinement was observed in a plasma experiment [28] and a good fit was obtained with a q-distribution with index $q = 2$ (in our notations) [29]. This confinement was justified by a lack of ergodicity in the system [30]. One can therefore interpret the Tsallis distributions as an attempt to take into account incomplete relaxation and non-ergodicity in systems with long-range interactions. In this interpretation, the index q could be a measure of mixing[8]. If we assume that the system mixes efficiently, then $q = 1$ and we get the Lynden-Bell theory. If the system does not mix well, the Lynden-Bell theory fails and $q \neq 1$. Since the value of the q parameter depends on the efficiency of mixing (which is not known a priori), it appears difficult to determine its value from first principles. Furthermore, its value can change from case to case since the degree of mixing can vary depending on the initial condition (some systems can mix well and others less). Finally, we can argue that the Tsallis entropy is just one generalized entropy among many others and that it may not be universal [36]. It may just describe a special type of non-ergodic behavior but not all of them. In fact, non-ergodic effects can be so complicated that it is hard to believe that they can be encapsulated in a simple functional such as the Tsallis functional or any other [30,25]. Nevertheless, we must recognize that some QSSs can be well-fitted by q-distributions. Even more strikingly, following the suggestion of [26], Campa *et al.* [37] demonstrated numerically that, during the collisional regime, the time dependent distribution $f(v,t)$ is still very well-fitted by $q(t)$-distributions with a time-dependent index. When the index reaches a critical value $q_{crit}(U)$ (predicted by the theory [26,37]), the distribution function becomes Vlasov

[4] Latora *et al.* [14] find that the Largest Lyapunov exponent for the QSS tends to zero. In this sense, mixing is negligible and one expects anomalies in the relaxation process. This is fully consistent with the idea of incomplete relaxation and inefficient mixing introduced by Lynden-Bell [20] and further discussed by Chavanis [25,18,26].

[5] Quoting Einstein [32] and Cohen [33], Latora *et al.* [14] argued that standard statistical mechanics fails when *the dynamics plays a nontrivial role* (e.g. long-range correlations or fractal structures in phase space). In our point of view, this is a correct interpretation although standard thermodynamics should refer here to Lynden-Bell's theory, which is the proper Boltzmann approach applied to the Vlasov equation. This subtlety is not addressed in the paper of Latora *et al.* [14] since they did not know the theory of Lynden-Bell at that time. Yet, their general comment can be applied to Lynden-Bell's theory as well: if the dynamics is nontrivial and the system does not mix well, standard (Lynden-Bell) statistical mechanics fails.

[6] For $M_0 = 1$, this differs from the numerical results of Latora *et al.* [14]. However, Campa *et al.* [34] show that the ordinary waterbag initial condition leads to the presence of large sample to sample fluctuations so that many averages are necessary. They proposed to use isotropic waterbag distributions to reduce the fluctuations.

[7] Let us be more precise: (i) For $M_0 = 1$, an isotropic waterbag distribution violently relaxes towards a q-distribution with $q = 3$ [34]; (ii) For $M_0 = 0$, a waterbag distribution is Vlasov stable and does not undergo violent relaxation (it is already the Lynden-Bell state). However, in the collisional regime (due to finite N effects), it becomes a q-distribution with $q = 3$ [17,34]; (iii) for intermediate values of M_0, the system violently relaxes towards the Lynden-Bell distribution [19,34].

[8] This interpretation was proposed by one of the authors in several papers [35,18,26] and it may be more accurate than the usual interpretation: "q is a measure of nonextensivity" [3].

unstable and a dynamical phase transition from the homogeneous phase (non-magnetized) to the inhomogeneous phase (magnetized) is triggered. This explains previous observations on the evolution of the magnetization $M(t)$ [14,17,34]. Interestingly, a very similar behavior has been found by Taruya & Sakagami [38] for self-gravitating systems[9].

In view of these results, it is interesting to study in more detail the structure and the stability of q-distributions. Note that q-distributions correspond to what have been called stellar polytropes in astrophysics [27]. They were introduced long ago by Eddington [40] as particular stationary solutions of the Vlasov equation. They were used to construct simple self-consistent mathematical models of galaxies. At some time, they were found to provide a reasonable fit of some observed star clusters, the so-called Plummer [41] model. Improved observation of globular clusters and galaxies showed that the fit is not perfect and more realistic models have been introduced since then [27]. However, stellar polytropes are still important for historical reasons and for their mathematical simplicity. The stability of polytropic distributions is an old problem in stellar dynamics [27]. It has been reconsidered recently, for box-confined systems, by Taruya & Sakagami [42-44] in the framework of Tsallis generalized thermodynamics and by Chavanis *et al.* [45,35,46,47,39] in relation to their nonlinear dynamical stability with respect to the Euler and Vlasov equations. It is therefore interesting to extend these studies to the case of the HMF model. For the moment, only spatially homogeneous polytropic distributions have been considered [9,48]. In the present paper, we extend the analysis to spatially *inhomogeneous* polytropes. Specifically, we study the maximization of the Tsallis functional at fixed mass and energy and plot the corresponding caloric curves. We give a thermodynamical and a dynamical interpretation of this variational principle. We find the existence of a critical polytropic index $q_c = 3$ (where results are analytical) which plays the role of a canonical tricritical point separating first and second order phase transitions in the canonical ensemble and marking the onset of negative specific heats in the microcanonical ensemble (there also exists a microcanonical tricritical point at $q \simeq 16.9$ and a microcanonical critical point at $q \simeq 6.55$). Interestingly, this critical value $q_c = 3$ turns out to be the one observed by Campa *al.* [34] in their numerical simulations. Then, we apply our theory to the situation considered by Antoni & Ruffo [8]. We find that the structure of their numerical caloric curve $T(U)$ close to the critical energy can be explained naturally if we assume that the QSSs in this region are polytropes with the critical index $q_c = 3$ (this result is specifically discussed in Sec. 7.2). This yields a transition energy $U_c' = 5/8$ lower than $U_c = 3/4$ and a region of negative specific heats in the curve $T(U)$ that are in qualitative agreement with the numerical results (the agreement could be improved by allowing q to deviate slightly from the critical value $q_c = 3$). These behaviors had never been explained since the original paper of Antoni & Ruffo [8]. We provide a plausible explanation in terms of Tsallis (polytropic) distributions. We qualitatively justify the occurence of polytropic distributions with a compact support in terms of incomplete relaxation. Furthermore, the index selected by the system appears to be the critical one (or close to it). This is the first time that a sort of prediction of the q index is made in that context. However, our approach does not explain everything and just opens a direction of research. Indeed, one has first to confirm the results by more detailed comparisons with numerical simulations and, in case of agreement, try to understand why critical polytropes are selected by the system and if this is a general feature.

[9] There is, however, a crucial difference in the interpretation. Taruya & Sakagami [38] interpret the instability in terms of Tsallis generalized thermodynamics while Campa *et al.* [37] interpret it in terms of Vlasov dynamical instability [39].

2 Interpretations of the Tsallis functionals

In order to motivate our study of polytropes, we shall first recall different interpretations of the Tsallis functionals that have been given previously by one of the authors [47,49].

2.1 Thermodynamical interpretation

There is no reason to describe the QSSs that emerge in Hamiltonian systems with long-range interactions in terms of Boltzmann statistical mechanics since they correspond to out-of-equilibrium structures (in the usual sense). The QSSs are formed during the collisionless regime while Boltzmann statistical equilibrium is reached on a much longer timescale at the end of the collisional regime. Fundamentally, the QSSs are stable steady states of the Vlasov equation (on a coarse-grained scale) and they should be described by Lynden-Bell's statistical mechanics. However, Lynden-Bell's theory, as any statistical theory, assumes efficient mixing and ergodicity. If the system does not mix well, the QSS will differ from the Lynden-Bell prediction (by definition). If we want to apply Tsallis generalized thermodynamics to that context, in order to take into account non ergodic effects and incomplete mixing, we must modify the Lynden-Bell entropy which is the Boltzmann entropy associated to the Vlasov equation[10]. Therefore, the proper q-entropy to consider is

$$S_q[\rho] = -\frac{1}{q-1}\int (\rho^q - \rho)\, d\eta d\mathbf{r} d\mathbf{v}. \qquad (1)$$

This entropy applies to the distribution $\rho(\mathbf{r}, \mathbf{v}, \eta)$ of phase levels η (see [49] for details) so as to take into account the

[10] Latora *et al.* [14] did not know the Lynden-Bell theory and proposed to replace the usual Boltzmann entropy $S[f] = -\int f \ln f\, d\mathbf{r}d\mathbf{v}$ by the q-entropy $S_q[f] = -\frac{1}{q-1}\int (f^q - f)\, d\mathbf{r}d\mathbf{v}$. However, as argued long ago in [30], this approach is in general incorrect since it does not take into account the constraints of the Vlasov equation. Furthermore, since $S_q[f]$ is rigorously conserved by the Vlasov equation (it is a particular Casimir), there is no thermodynamical reason to maximize it.

constraints of the Vlasov equation (Casimirs). For $q = 1$ (efficient mixing), we recover the Lynden-Bell entropy. For $q \neq 1$, this functional could describe incomplete violent relaxation and non-ergodic effects in the framework of Tsallis thermodynamics. Now, for two-levels initial conditions and in the non degenerate limit (this corresponds to the waterbag model with initial magnetization $M_0 = 1$ in the HMF model), the Lynden-Bell entropy takes a form similar to the Boltzmann entropy and the constraints reduce to the mass and the energy. In that case, the generalized Lynden-Bell entropy (1) reduces to

$$S_q[\overline{f}] = -\frac{1}{q-1}\int \left[\left(\frac{\overline{f}}{\eta_0}\right)^q - \frac{\overline{f}}{\eta_0}\right] d\mathbf{r}d\mathbf{v}. \qquad (2)$$

This is similar to the Tsallis entropy considered by Latora *et al.* [14] but it arises here for a different reason: note in particular the bar on $\overline{f}$ (coarse-grained distribution) and the presence of the initial phase level η_0. Note that $S_q[\overline{f}]$ is expected to increase while $S_q[f]$ is conserved. In this thermodynamical approach, the QSS is obtained by maximizing the Tsallis entropy at fixed mass and energy (microcanonical ensemble). This is expected to select the most probable state *under some dynamical constraints* (responsible for incomplete mixing) that are implicitly taken into account in the form of the entropy. The canonical ensemble has no justification in the present context but, as usual, it can be useful to provide a *sufficient* condition of microcanonical stability [50].

Since the Tsallis entropy (1) includes the Lynden-Bell entropy as a special case (for $q = 1$), it can give at least as good, or better, results. However, we would like to emphasize several limitations of Tsallis generalized thermodynamics: (i) at present, there is no theory predicting the value of q. This prediction is of course very difficult since q is related to non-ergodic effects. For the moment, q appears as a fitting parameter measuring the degree of mixing of a system; (ii) it is not clear that all non-ergodic processes can be described by the Tsallis entropy. Therefore, this functional is probably not universal. It may, however, describe a certain class of non-ergodic behaviors[11]; (iii) it is not clear that non-ergodic effects can be described by a simple entropic functional such as the Tsallis functional or any other. Maybe, a better approach is to consider the *dynamics of mixing* and develop kinetic theories and relaxation equations of the process of violent relaxation as suggested in [51,25,26,49]. This kinetic approach may be closer to the original ideas of Einstein [32] and Cohen [33].

[11] It has been shown that the Tsallis entropy satisfies a lot of axioms satisfied by the Boltzmann entropy. This makes this entropy very "natural" to generalize the Boltzmann entropy. However, the axiomatic approach may not be the best justification of an entropy. The original combinatorial approach of Boltzmann seems to be more relevant. The Boltzmann and the Lynden-Bell entropies can be derived from a combinatorial analysis by assuming that all the microstates are equiprobable. It would be interesting to derive the Tsallis entropy from a combinatorial analysis by putting some constraints on the availability of the microstates.

2.2 Dynamical interpretation

We would like to give another interpretation of Tsallis functional that is not related to thermodynamics and that does not suffer the limitations exposed above. It will show that the Tsallis formalism can be useful in a dynamical context, using a thermodynamical analogy [47,39,49].

It has been known for a long time that any distribution function of the form $f = f(\epsilon)$, where $\epsilon = v^2/2 + \Phi$ is the individual energy, is a steady state of the Vlasov equation [52]. In particular, q-distributions have been introduced long ago by Eddington [40] in astrophysics where they are called stellar polytropes[12]. It is also known that these distributions are critical points of a certain functional of the form

$$S[f] = -\int C(f)\, d\mathbf{r}d\mathbf{v}, \qquad (3)$$

where C is a convex function, at fixed mass and energy. Furthermore, if they are *maxima* of this functional, they are nonlinearly dynamically stable with respect to the Vlasov equation. As far as we know, this dynamical stability criterion was first stated by Ipser & Horwitz [54] in astrophysics. Furthermore, Ipser [55] introduced the functional $S = -\int f^{1+1/(n-3/2)}\, d\mathbf{r}d\mathbf{v}$ (in his notations) associated to stellar polytropes. This is nothing but the Tsallis functional[13].

Let us be more precise and more general. The maximization problem

$$\max_f \{S[f]\,|\,E[f] = E,\, M[f] = M\}, \qquad (4)$$

determines a steady state of the Vlasov equation of the form $f = f(\epsilon)$ with $f'(\epsilon) < 0$ that is nonlinearly dynamically stable. This has been stated by Ellis *et al.* [56] in 2D turbulence (for the 2D Euler equation) and by Ipser & Horwitz [54], Tremaine *et al.* [57] and Chavanis [39] in stellar dynamics. The maximization problem (4) is similar to a condition of microcanonical stability in thermodynamics. Therefore, we can develop a *thermodynamical analogy* [49] to investigate the nonlinear dynamical stability problem. In this analogy, S is called a pseudo entropy. Thus, the Tsallis functional is a particular pseudo entropy whose maximization at fixed mass and energy determines distributions (polytropes) that are nonlinearly dynamically stable with respect to the Vlasov equation [47,39].

[12] The connection between q-distributions and stellar polytropes was first mentioned by Plastino & Plastino [53]. A more detailed discussion has been given recently by Chavanis & Sire [47].

[13] Indeed, the second term in the Tsallis functional (11) is a constant (proportional to mass) and the first term coincides with the Ipser functional with the notation (18). As noted in [47], the Tsallis functional (11) is more convenient to take the limit $q \to 1$ (i.e. $n \to +\infty$) since it reduces to the Boltzmann functional while the Ipser functional takes a trivial form. Therefore, the Tsallis functional allows to make a continuous link between isothermal ($n = \infty$) and polytropic (n finite) distributions using L'Hôpital's rule.

The minimization problem

$$\min_f \{F[f] = E[f] - TS[f] \,|\, M[f] = M\}. \qquad (5)$$

also determines a steady state of the Vlasov equation that is nonlinearly dynamically stable. In fact, (4) and (5) have the same critical points. However, the criterion (5) is less refined than (4). Indeed, the minimization problem (5) is similar to a condition of canonical stability in thermodynamics. In this analogy, F is called a pseudo free energy. Now, it is a general result [50] that canonical stability implies microcanonical stability, but the reciprocal is wrong in case of ensembles inequivalence. Schematically: (5) $\Rightarrow$ (4). In the present dynamical context, this means that steady states of the Vlasov equation that are stable according to the criterion (5) are necessarily stable according to the more constrained criterion (4). However, there may exist steady states of the Vlasov equation that are stable according to (4) while they fail to satisfy (5). As shown in [39], this is the case for stellar polytropes with indices $3 < n < 5$ in astrophysics.

It can also be shown [49] that (5) is equivalent to

$$\min_\rho \{F[\rho] \,|\, M[\rho] = M\}, \qquad (6)$$

where

$$F = \frac{1}{2}\int \rho\Phi\, d\mathbf{r} + \int \rho \int^\rho \frac{p(\rho')}{\rho'^2}\, d\rho' d\mathbf{r}. \qquad (7)$$

More precisely, a distribution function $f(\mathbf{r},\mathbf{v})$ is solution of (5) iff the corresponding density profile $\rho(\mathbf{r})$ is solution of (6), where $p(\rho)$ is the equation of state determined by $C(f)$ (see [49] for more details). Finally, (6) is clearly equivalent to

$$\min_{\rho,\mathbf{u}} \{\mathcal{W}[\rho,\mathbf{u}] \,|\, M[\rho] = M\}, \qquad (8)$$

where

$$\mathcal{W} = \int \rho \int^\rho \frac{p(\rho')}{\rho'^2}\, d\rho' d\mathbf{r} + \frac{1}{2}\int \rho\Phi\, d\mathbf{r} + \int \rho \frac{\mathbf{u}^2}{2}\, d\mathbf{r}. \qquad (9)$$

Now, it can be shown that this minimization problem determines a steady solution of the barotropic Euler equation that is formally nonlinearly dynamically stable [27]. From the implication (8) $\Leftrightarrow$ (6) $\Leftrightarrow$ (5) $\Rightarrow$ (4), we conclude that a distribution $f(\mathbf{r},\mathbf{v})$ is stable with respect to the Vlasov equation [according to (4)] if the corresponding density profile $\rho(\mathbf{r})$ is stable with respect to the Euler equation [according to (8)]. As shown in [39], this provides a nonlinear generalization of the Antonov first law in astrophysics: "a spherical galaxy $f = f(\epsilon)$ with $f'(\epsilon) < 0$ is nonlinearly dynamically stable with respect to the Vlasov-Poisson system if the corresponding barotropic star is nonlinearly dynamically stable with respect to the Euler-Poisson system". Interestingly, this also provides a new interpretation [39] of this law in terms of ensembles inequivalence. Indeed, the Antonov first law has the same status as the fact that "canonical stability implies microcanonical stability" in thermodynamics.

Remark: the "microcanonical" criterion (4) provides itself just a sufficient condition of nonlinear dynamical stability. There exists an even more refined criterion of nonlinear dynamical stability taking into account the conservation of all the Casimirs (see discussion in [48]).

2.3 Generalized H-functions and selective decay

A generalized H-function is a functional of the coarse-grained distribution function $\overline{f}(\mathbf{r},\mathbf{v},t)$ of the form

$$H[\overline{f}] = -\int C(\overline{f})\, d\mathbf{r}d\mathbf{v}, \qquad (10)$$

where C is any convex function. Tremaine *et al.* [57] have shown that the generalized H-functions increase during violent relaxation in the sense that $H(t) \geq H(0)$ for any time $t \geq 0$ where it is assumed that the initial distribution function is not mixed so that $\overline{f}(\mathbf{r},\mathbf{v},t=0) = f(\mathbf{r},\mathbf{v},t=0)$[14]. By contrast, the energy $E[\overline{f}]$ and $M[\overline{f}]$ and the mass calculated with the coarse-grained distribution function are approximately conserved. This suggests a phenomenological *generalized selective decay principle* (for $-H$): "due to mixing, the system may tend to a QSS that maximizes a certain H-function (non universal) at fixed mass and energy" [49][15]. In that context, the Tsallis functionals $H[\overline{f}] = -\frac{1}{q-1}\int(\overline{f}^q - \overline{f})\, d\mathbf{r}d\mathbf{v}$ can be interpreted as particular generalized H-functions [49].

3 Polytropic distributions: general theory

For any of the reasons exposed previously, we think that it is useful to study polytropic (Tsallis) distribution functions and investigate their stability through the variational problems (4) and (5). We first develop a general theory of polytropes following the lines of [46,47]. It will be applied specifically to the HMF model in Sec. 4.

3.1 Polytropic distributions in phase space

Let us consider the Tsallis functional

$$S = -\frac{1}{q-1}\int (f^q - f_0^{q-1} f)\, d\mathbf{r}d\mathbf{v}. \qquad (11)$$

We have introduced a constant f_0 in order to make the expression homogeneous. This constant will play no role in the following since the last term is proportional to the

[14] Note that the time evolution of the generalized H-functions is not necessarily monotonic (nothing is implied concerning the relative values of $H(t)$ and $H(t')$ for $t, t' > 0$).

[15] The close relationship between this phenomenological principle and the criterion of nonlinear dynamical stability (4), as well as the limitations of this phenomenological principle, are discussed in detail in [25,49].

mass that is conserved. Therefore, we could equally work with the Ipser functional

$$S=-\frac{1}{q-1}\int f^q\,d\mathbf{r}d\mathbf{v}, \tag{12}$$

but the first expression allows us to make the connection with isothermal distributions when $q\to 1$. Indeed, for $q\to 1$, we recover the Boltzmann functional

$$S=-\int f\ln\left(\frac{f}{f_0}\right)\,d\mathbf{r}d\mathbf{v}. \tag{13}$$

We shall consider the maximization of the Tsallis functional at fixed energy and mass

$$E=\int f\frac{v^2}{2}\,d\mathbf{r}d\mathbf{v}+\frac{1}{2}\int\rho\Phi\,d\mathbf{r}, \tag{14}$$

$$M=\int\rho\,d\mathbf{r}. \tag{15}$$

Some interpretations of this variational problem have been given in Sec. 2. Here, S is either a generalized entropy (thermodynamical interpretation) or a pseudo entropy (dynamical interpretation). By an abuse of language, and to simplify the terminology, we shall call it simply an entropy. We will work in a space of dimension d since our formalism can have application for different systems.

The critical points of entropy at fixed energy and mass are determined by the condition

$$\delta S-\beta\delta E-\alpha\delta M=0, \tag{16}$$

where $\beta=1/T$ and α are Lagrange multipliers (T is the inverse temperature and α the chemical potential). This yields the q-distributions (or polytropic distributions):

$$f(\mathbf{r},\mathbf{v})=\left\{\mu-\frac{(q-1)\beta}{q}\left[\frac{v^2}{2}+\Phi(\mathbf{r})\right]\right\}_+^{1/(q-1)}, \tag{17}$$

where $\mu=[f_0^{q-1}-(q-1)\alpha]/q$. The notation $[x]_+=x$ if $x\geq 0$ and $[x]_+=0$ if $x\leq 0$. As is customary in astrophysics, we define the polytropic index n by the relation[16]

$$n=\frac{d}{2}+\frac{1}{q-1}. \tag{18}$$

The distribution function $f(\mathbf{r},\mathbf{v})$ depends only on the individual energy $\epsilon=v^2/2+\Phi(\mathbf{r})$, i.e. $f=f(\epsilon)$. Therefore, it is a steady state of the Vlasov equation. We shall consider $q>0$ so that $C(f)$ is convex and $\beta>0$ so that $f'(\epsilon)<0$, which corresponds to the physical situation. For $n=d/2$ ($q\to+\infty$), we recover the Fermi distribution [18]. For $n\to+\infty$ ($q\to 1$), we recover the isothermal distribution.

We need to distinguish two cases depending on the sign of $q-1$. (i) For $q>1$ ($n\geq d/2$), the distribution function can be written

$$f=A(\epsilon_m-\epsilon)_+^{\frac{1}{q-1}}, \tag{19}$$

where we have set $A=[\beta(q-1)/q]^{\frac{1}{q-1}}$ and $\epsilon_m=q\mu/[\beta(q-1)]$. Such distributions have a compact support in phase space since they vanish at $\epsilon=\epsilon_m$. At a given position, the distribution function vanishes for $v\geq v_m(\mathbf{r})=\sqrt{2(\epsilon_m-\Phi(\mathbf{r}))}$. (ii) For $0<q<1$, the distribution function can be written

$$f=A(\epsilon_0+\epsilon)^{\frac{1}{q-1}}, \tag{20}$$

where we have set $A=[\beta(1-q)/q]^{\frac{1}{q-1}}$ and $\epsilon_0=q\mu/[\beta(1-q)]$. Such distributions are defined for all velocities. At a given position, the distribution function behaves, for large velocities, as $f\sim v^{-2/(1-q)}\sim v^{-(d-2n)}$. We shall only consider distribution functions for which the density and the pressure

$$\rho=\int f\,d\mathbf{v},\qquad p=\frac{1}{d}\int fv^2\,d\mathbf{v}, \tag{21}$$

are finite. This implies $d/(d+2)<q<1$ ($n<-1$).

3.2 Polytropic equation of state

For any distribution function of the form $f=f(\epsilon)$, the density and the pressure are functions of $\Phi(\mathbf{r})$ such that $\rho=\rho[\Phi(\mathbf{r})]$ and $p=p[\Phi(\mathbf{r})]$. Eliminating $\Phi(\mathbf{r})$ between these expressions, we obtain a barotropic equation of state $p(\mathbf{r})=p[\rho(\mathbf{r})]$. Furthermore, it is easy to see that $f=f(\epsilon)$ implies the condition of hydrostatic equilibrium (see Appendix A):

$$\nabla p+\rho\nabla\Phi=\mathbf{0}. \tag{22}$$

Let us determine the equation of state corresponding to the polytropic distribution (17). For $n\geq d/2$, the density and the pressure can be expressed as (see Appendix B):

$$\rho=AS_d(\epsilon_m-\Phi)^n 2^{d/2-1}\frac{\Gamma(d/2)\Gamma(1-d/2+n)}{\Gamma(n+1)}, \tag{23}$$

$$p=\frac{AS_d}{n+1}(\epsilon_m-\Phi)^{n+1}2^{d/2-1}\frac{\Gamma(d/2)\Gamma(1-d/2+n)}{\Gamma(n+1)}, \tag{24}$$

where $\Gamma(x)$ denotes the Gamma function and S_d the surface of a unit sphere in d dimensions. For $n<-1$, the density and the pressure can be expressed as (see Appendix B):

$$\rho=AS_d(\epsilon_0+\Phi)^n 2^{d/2-1}\frac{\Gamma(-n)\Gamma(d/2)}{\Gamma(d/2-n)}, \tag{25}$$

$$p=-\frac{AS_d}{n+1}(\epsilon_0+\Phi)^{n+1}2^{d/2-1}\frac{\Gamma(-n)\Gamma(d/2)}{\Gamma(d/2-n)}. \tag{26}$$

Eliminating the field $\Phi(\mathbf{r})$ between the expressions (23)-(24) and (25)-(26), one finds that

$$p=K\rho^\gamma,\qquad \gamma=1+\frac{1}{n}. \tag{27}$$

[16] This relation is sometimes presented as a "fundamental" relation relating the q-parameter to the polytropic index n [3]. In our sense, this is just a definition of notations, no more.

This is the classical polytropic equation of state. This is the reason why the distributions (17) are called polytropic distributions. Furthermore, γ is the ordinary polytropic index and n is a polytropic index commonly used in astrophysics [58]. The polytropic constant K is given for $n \geq d/2$ by

$$K = \frac{1}{n+1}\left\{AS_d 2^{d/2-1}\frac{\Gamma(d/2)\Gamma(1-d/2+n)}{\Gamma(n+1)}\right\}^{-\frac{1}{n}} \quad (28)$$

and for $n < -1$ by

$$K = -\frac{1}{n+1}\left\{AS_d 2^{d/2-1}\frac{\Gamma(-n)\Gamma(d/2)}{\Gamma(d/2-n)}\right\}^{-\frac{1}{n}}. \quad (29)$$

The polytropic constant K plays the role of the temperature T_{iso} in isothermal systems ($q = 1$, $n = \infty$, $\gamma = 1$) and it is sometimes called a "polytropic temperature". For polytropic distributions, the relation between the polytropic temperature K and the thermodynamical temperature $T = 1/\beta$ is

$$T = C_n K^{\frac{2n}{2n-d}}, \quad (30)$$

where C_n is given for $n \geq d/2$ by

$$C_n = \frac{2(n+1)^{\frac{2n}{2n-d}}}{2n-d+2}\left[S_d 2^{d/2-1}\frac{\Gamma(d/2)\Gamma(1-d/2+n)}{\Gamma(n+1)}\right]^{\frac{2}{2n-d}} \quad (31)$$

and for $n < -1$ by

$$C_n = \frac{2[-(n+1)]^{\frac{2n}{2n-d}}}{-2n+d-2}\left[S_d 2^{d/2-1}\frac{\Gamma(d/2)\Gamma(-n)}{\Gamma(d/2-n)}\right]^{\frac{2}{2n-d}}. \quad (32)$$

We note that K is a monotonically increasing function of T. This remark will have some importance in the following.

3.3 Polytropic distributions in physical space

The density is obtained by integrating Eq. (17) on the velocity leading to Eqs. (23) and (25). Using Eqs. (28) and (29), we find that the density is related to the potential $\Phi(\mathbf{r})$ by

$$\rho(\mathbf{r}) = \left[\lambda - \frac{\gamma-1}{K\gamma}\Phi(\mathbf{r})\right]_+^{\frac{1}{\gamma-1}}, \quad (33)$$

where $\lambda = \epsilon_m/(K(n+1))$ for $n \geq d/2$ and $\lambda = \epsilon_0/(-K(n+1))$ for $n < -1$. As noted in [47], the polytropic distribution in phase space $f = f(\epsilon)$ given by Eq. (17) has the same mathematical form as the polytropic distribution in physical space $\rho = \rho(\Phi)$ given by Eq. (33) with γ playing the role of q and K playing the role of $T = 1/\beta$. In this correspondence, γ is related to q by Eqs. (27) and (18) leading to $\gamma = ((d+2)q-d)/(dq-d+2)$ and K is related to T by Eq. (30). Polytropic distributions (including the isothermal one) are apparently the only distributions for which $f(\epsilon)$ and $\rho(\Phi)$ have the same mathematical form.

3.4 Other expressions of the distribution function

We can write the polytropic distribution function (17) in different forms that all have their own interest. This will show that different notions of "temperature" exist for polytropic distributions.

(i) *Thermodynamical temperature* $T = 1/\beta$: the polytropic distribution (17) directly comes from the variational principle (16). Therefore, $\beta = 1/T$ is the Lagrange multiplier associated with the conservation of energy. This is the proper thermodynamical temperature to consider, i.e. $\beta = (\partial S/\partial E)_M$ is the conjugate of the energy with respect to the entropy. Note, however, that $T = 1/\beta$ does not have the dimension of an ordinary temperature (squared velocity).

(ii) *Dimensional temperature* $\theta = 1/b$: we can define a quantity that has the dimension of a temperature (squared velocity) by setting $b = \beta/q\mu$. If we define furthermore $f_* = \mu^{1/(q-1)}$, the polytropic distribution (17) can be rewritten

$$f = f_*\left[1 - b(q-1)\epsilon\right]_+^{\frac{1}{q-1}}. \quad (34)$$

Comparing Eq. (34) with Eqs. (19) and (20) we find that $\epsilon_m = 1/[b(q-1)]$ and $A = f_*/\epsilon_m^{1/(q-1)}$ for $n \geq d/2$ and $\epsilon_0 = 1/[b(1-q)]$ and $A = f_*/\epsilon_0^{1/(q-1)}$ for $n < -1$. Substituting these expressions in Eqs. (23) and (25), we find that the relation between the density and the potential can be written

$$\rho = \rho_*\left[1 - b(q-1)\Phi\right]_+^n, \quad (35)$$

where ρ_* is given for $n \geq d/2$ by

$$\rho_* = \frac{S_d}{2}f_*\left(\frac{2n-d}{b}\right)^{d/2}\frac{\Gamma(d/2)\Gamma(1-d/2+n)}{\Gamma(n+1)}, \quad (36)$$

and for $n < -1$ by

$$\rho_* = \frac{S_d}{2}f_*\left(\frac{d-2n}{b}\right)^{d/2}\frac{\Gamma(d/2)\Gamma(-n)}{\Gamma(d/2-n)}. \quad (37)$$

(iii) *Polytropic temperature* K: eliminating the potential between Eqs. (19) and (23), and between Eqs. (20) and (25), and using Eqs. (28) and (29), we can express the distribution function in terms of the density according to

$$f = \frac{1}{Z}\left[\rho(\mathbf{r})^{1/n} - \frac{v^2/2}{(n+1)K}\right]_+^{n-d/2}, \quad (38)$$

where Z is given for $n \geq d/2$ by

$$Z = S_d 2^{d/2-1}\frac{\Gamma(d/2)\Gamma(1-d/2+n)}{\Gamma(n+1)}[K(n+1)]^{d/2}, \quad (39)$$

and for $n < -1$ by

$$Z = S_d 2^{d/2-1} \frac{\Gamma(-n)\Gamma(d/2)}{\Gamma(d/2-n)} [-K(n+1)]^{d/2}. \quad (40)$$

This is the polytropic counterpart of the isothermal distribution. The constant K plays a role similar to the temperature T_{iso} in an isothermal distribution. In particular, it is uniform in a polytropic distribution as is the temperature in an isothermal system. This is why K is sometimes called a polytropic temperature.

(iv) *Kinetic temperature* $T_{kin}(\mathbf{r})$: the kinetic temperature is defined by

$$T_{kin}(\mathbf{r}) = \frac{1}{d}\langle v^2\rangle(\mathbf{r}) = p(\mathbf{r})/\rho(\mathbf{r}). \quad (41)$$

For a polytropic distribution, using the equation of state (27), we get

$$T_{kin}(\mathbf{r}) = K\rho(\mathbf{r})^{\gamma-1}. \quad (42)$$

For a spatially inhomogeneous polytrope, the kinetic temperature $T_{kin}(\mathbf{r})$ is position dependent and differs from the thermodynamical temperature $T = 1/\beta$. The velocity of sound $c_s^2 = p'(\rho)$ is given by

$$c_s^2(\mathbf{r}) = K\gamma\rho(\mathbf{r})^{\gamma-1} = \gamma T_{kin}(\mathbf{r}). \quad (43)$$

It is also position dependent and differs from the velocity dispersion (they differ by a factor γ). Using Eq. (41), the distribution function (38) can be written

$$f = B_n \frac{\rho(\mathbf{r})}{[2\pi T_{kin}(\mathbf{r})]^{d/2}} \left[1 - \frac{v^2/2}{(n+1)T_{kin}(\mathbf{r})}\right]_+^{n-d/2}, \quad (44)$$

$$B_n = \frac{\Gamma(n+1)}{\Gamma(1-d/2+n)(n+1)^{d/2}}, \quad (n \geq d/2) \quad (45)$$

$$B_n = \frac{\Gamma(d/2-n)}{\Gamma(-n)[-(n+1)]^{d/2}} \quad (n < -1). \quad (46)$$

Note that for $n \geq d/2$, the maximum velocity can be expressed in terms of the kinetic temperature by

$$v_m(\mathbf{r}) = \sqrt{2(n+1)T_{kin}(\mathbf{r})}. \quad (47)$$

Using $\Gamma(z+a)/\Gamma(z) \sim z^a$ for $z \to +\infty$, we recover the isothermal distribution for $n \to +\infty$. On the other hand, from Eqs. (42) and (33), we immediately get $T_{kin}(\mathbf{r}) = K(\lambda - (\gamma-1)\Phi(\mathbf{r})/K\gamma)$ so that

$$\nabla T_{kin} = -\frac{\gamma-1}{\gamma}\nabla\Phi. \quad (48)$$

This shows that, for a polytropic distribution, the kinetic temperature (velocity dispersion) is a linear function of the potential[17]. The coefficient of proportionality is related to the polytropic index by $(\gamma-1)/\gamma = 1/(n+1) = 2(q-1)/[(d+2)q-d]$. The relation (48) can also be obtained directly from Eq. (19) [or Eq. (20)] noting that

$$f = A(\epsilon_m - \Phi)^{n-d/2} \left[1 - \frac{v^2/2}{\epsilon_m - \Phi}\right]_+^{n-d/2}, \quad (49)$$

and comparing with Eq. (44).

(v) *Energy excitation temperature* $T(\epsilon)$: for any distribution function of the form $f = f(\epsilon)$, one may define a local energy dependent excitation temperature by the relation

$$\frac{1}{T(\epsilon)} = -\frac{d\ln f}{d\epsilon}. \quad (50)$$

For the isothermal distribution, $T(\epsilon)$ coincides with the usual temperature T_{iso}. For the polytropic distribution (17), $T(\epsilon) = q\mu/\beta - (q-1)\epsilon$. This excitation temperature has a constant gradient $dT/d\epsilon = 1-q$ related to the polytropic index. The other parameter μ is related to the value of the energy where the temperature reaches zero.

3.5 Entropy and free energy in physical space

Substituting the polytropic distribution function (38) in the Tsallis entropy (11), we find after some calculations (see Appendix C) that

$$S = -\left(n - \frac{d}{2}\right)\left(\beta\int p\,d\mathbf{r} - f_0^{q-1}M\right). \quad (51)$$

On the other hand, the energy (14) can be written

$$E = \frac{d}{2}\int p\,d\mathbf{r} + \frac{1}{2}\int\rho\Phi\,d\mathbf{r}. \quad (52)$$

Therefore, the free energy $F = E - TS$ is given by

$$F = \frac{1}{2}\int\rho\Phi\,d\mathbf{r} + n\int p\,d\mathbf{r}, \quad (53)$$

up to unimportant constant terms. It can also be written

$$F = \frac{1}{2}\int\rho\Phi\,d\mathbf{r} + \frac{K}{\gamma-1}\int\left(\rho^\gamma - \rho_0^{\gamma-1}\rho\right)d\mathbf{r}, \quad (54)$$

where

$$\rho_0^{\gamma-1} = \frac{\gamma-1}{K}\frac{T}{q-1}f_0^{q-1}. \quad (55)$$

This can be viewed as a free energy $F = E - KS$ associated with a Tsallis entropy in physical space $S = \frac{1}{\gamma-1}\int(\rho^\gamma - \rho_0^{\gamma-1}\rho)\,d\mathbf{r}$ where γ plays the role of q and K the role of T. Again, it is interesting to note that, for polytropes, the free energy in phase space $F[f]$ has a form similar to the free energy in position space $F[\rho]$ [47].

[17] For any distribution of the form $f = f(\epsilon)$, we have $\rho = \rho(\Phi)$ and $p = p(\Phi)$ so that the kinetic temperature (velocity dispersion) $T_{kin} = p/\rho$ is a function $T_{kin} = T_{kin}(\Phi)$ of the potential. For a polytropic distribution function, this relation turns out to be linear.

4 Application to the HMF model

4.1 Generalities

The HMF model is a system of N particles of unit mass $m = 1$ moving on a circle and interacting via a cosine potential. The dynamics of these particles is governed by the Hamilton equations [6,8,9]:

$$\frac{d\theta_i}{dt} = \frac{\partial H}{\partial v_i}, \qquad \frac{dv_i}{dt} = -\frac{\partial H}{\partial \theta_i},$$
$$H = \frac{1}{2}\sum_{i=1}^{N} v_i^2 - \frac{k}{4\pi}\sum_{i\neq j}\cos(\theta_i - \theta_j), \tag{56}$$

where $\theta_i \in [-\pi, \pi]$ and $-\infty < v_i < \infty$ denote the position (angle) and the velocity of particle i and k is the coupling constant. The thermodynamic limit corresponds to $N \to +\infty$ in such a way that the rescaled energy $\epsilon = 8\pi E/kM^2$ remains of order unity (this amounts to taking $k \sim 1/N$ and $E/N \sim 1$). In that limit, the mean field approximation becomes exact. The total mass and total energy are given by

$$M = \int \rho\, d\theta, \tag{57}$$

$$E = \int f\frac{v^2}{2}\, d\theta dv + \frac{1}{2}\int \rho\Phi\, d\theta = E_{kin} + W, \tag{58}$$

where $f(\theta, v)$ is the distribution function, $\rho(\theta) = \int f\, dv$ the density, E_{kin} the kinetic energy and W the potential energy. The potential is related to the density by

$$\Phi(\theta) = -\frac{k}{2\pi}\int_0^{2\pi} \cos(\theta - \theta')\rho(\theta')\, d\theta', \tag{59}$$

and the mean force acting on a particle located in θ is $\langle F\rangle = -\Phi'(\theta)$. For a cosine interaction, the potential can be written

$$\Phi(\theta) = -B_x\cos\theta - B_y\sin\theta, \tag{60}$$

where

$$B_x = \frac{k}{2\pi}\int_0^{2\pi}\rho(\theta)\cos\theta\, d\theta, \tag{61}$$

$$B_y = \frac{k}{2\pi}\int_0^{2\pi}\rho(\theta)\sin\theta\, d\theta, \tag{62}$$

are the two components of the magnetization vector up to a multiplicative factor (note the change of sign with respect to [9]). Substituting Eq. (60) in the potential energy (58), we find that the energy can be rewritten

$$E = \int f\frac{v^2}{2}\, d\theta dv - \frac{\pi B^2}{k}, \tag{63}$$

where $B^2 = B_x^2 + B_y^2$. It is a nice property of the HMF model that the potential energy can be expressed in terms of the order parameter B played here by the magnetization. This is not the case for more complex potentials such as the gravitational potential. Note, finally, that the kinetic temperature can be expressed in terms of the pressure (21) so that

$$E = \frac{1}{2}\int_0^{2\pi} p\, d\theta - \frac{\pi B^2}{k} = E_{kin} + W. \tag{64}$$

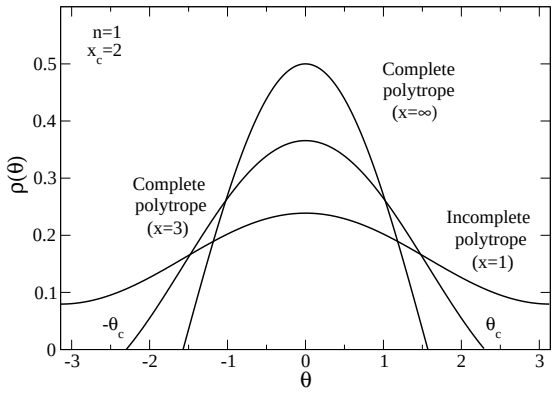

Fig. 1. Density profile for the polytropes $n = 1$. We have represented incomplete ($x > x_c$) and complete ($x < x_c$) polytropes.

4.2 Complete and incomplete polytropes

Let us now study polytropic distributions in the context of the HMF model. According to Eq. (33), their density profile is given by

$$\rho(\theta) = A\left[1 - \frac{\gamma - 1}{K\gamma A^{\gamma-1}}\Phi(\theta)\right]_+^{\frac{1}{\gamma-1}}, \tag{65}$$

where $A = \lambda^{1/(\gamma-1)}$. We can assume without loss of generality that the distribution is symmetrical with respect to the x axis ($\theta = 0$). In that case, the potential can be written

$$\Phi = -B\cos\theta, \tag{66}$$

where

$$B = \frac{k}{2\pi}\int_0^{2\pi}\rho(\theta)\cos\theta\, d\theta, \tag{67}$$

is the magnetization ($B_y = 0$ and $B = B_x$). The density profile can be rewritten

$$\rho(\theta) = A\left[1 + \frac{\gamma - 1}{\gamma}x\cos\theta\right]_+^{\frac{1}{\gamma-1}}, \tag{68}$$

where

$$x = \frac{B}{KA^{\gamma-1}}. \tag{69}$$

For $\gamma \to 1$, we recover the isothermal distribution (20) and the relation $x = \beta B$ of [9]. For $x > 0$, the density profile is concentrated around $\theta = 0$ and for $x < 0$, we get a symmetrical density profile concentrated around $\theta = \pi$.

Like for the gravitational interaction, we can have complete or incomplete polytropes [46]. By definition, complete polytropes have a compact support (the density

drops to zero at $\theta_c < \pi$) while incomplete polytropes extend over the whole domain. Let us first consider the case $n \geq 1/2$ (i.e. $1 \leq \gamma \leq 3$). The density profile can be written

$$\rho(\theta) = A\left(1+\frac{x}{n+1}\cos\theta\right)_+^n. \quad (70)$$

By symmetry, we can restrict ourselves to the interval $0 \leq \theta \leq \pi$ and to $x \geq 0$. The density profile is monotonically decreasing and it has a compact support iff the term in parenthesis is negative for $\theta = \pi$. This occurs iff

$$x > x_c \equiv n+1 = \frac{\gamma}{\gamma-1}. \quad (71)$$

If $x < x_c$, the density is strictly positive on $0 \leq \theta \leq \pi$ (incomplete polytrope). If $x > x_c$, the density vanishes for $\theta \geq \theta_c$ (complete polytrope) such that

$$1+\frac{1}{n+1}x\cos\theta_c = 0. \quad (72)$$

Therefore, θ_c is given by

$$\theta_c = \arccos\left(-\frac{x_c}{x}\right). \quad (73)$$

Some typical polytropic profiles are represented in Fig. 1. We now consider the case $n < -1$ (i.e. $0 \leq \gamma \leq 1$). The density profile can be written

$$\rho(\theta) = \frac{A}{\left(1-\frac{x}{|n+1|}\cos\theta\right)^{|n|}}, \quad (74)$$

and the solution is physical iff

$$x < x_* = -(n+1) = -\frac{\gamma}{\gamma-1}. \quad (75)$$

In that case, the polytropes are always incomplete.

4.3 The magnetization and the polytropic temperature

For the density profile (68), the mass and the magnetization are given by

$$M = A\int_0^{2\pi}\left(1+\frac{\gamma-1}{\gamma}x\cos\theta\right)_+^{\frac{1}{\gamma-1}} d\theta, \quad (76)$$

$$B = \frac{kA}{2\pi}\int_0^{2\pi}\left(1+\frac{\gamma-1}{\gamma}x\cos\theta\right)_+^{\frac{1}{\gamma-1}}\cos\theta\, d\theta. \quad (77)$$

It is useful to introduce the γ-deformed Bessel functions

$$I_{\gamma,m}(x) = \frac{1}{2\pi}\int_0^{2\pi}\left(1+\frac{\gamma-1}{\gamma}x\cos\theta\right)_+^{\frac{1}{\gamma-1}}\cos(m\theta)\, d\theta. \quad (78)$$

For $\gamma \to 1$, we recover the Bessel functions $I_m(x)$. For $1 \leq \gamma \leq 3$ ($n \geq 1/2$) and $x < x_c$, we have

$$I_{\gamma,m}(x) = \frac{1}{2\pi}\int_{-\pi}^{\pi}\left(1+\frac{\gamma-1}{\gamma}x\cos\theta\right)^{\frac{1}{\gamma-1}}\cos(m\theta)\, d\theta, \quad (79)$$

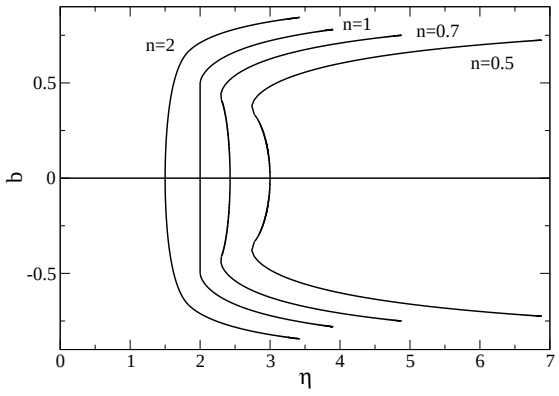

Fig. 2. Magnetization as a function of the polytropic temperature for $n \geq 1/2$.

and for $x > x_c$, we have

$$I_{\gamma,m}(x) = \frac{1}{2\pi}\int_{-\theta_c}^{\theta_c}\left(1+\frac{\gamma-1}{\gamma}x\cos\theta\right)^{\frac{1}{\gamma-1}}\cos(m\theta)\, d\theta. \quad (80)$$

We also have $I_{\gamma,m}(-x) = I_{\gamma,m}(x)$ if m is even and $I_{\gamma,m}(-x) = -I_{\gamma,m}(x)$ if m is odd. In terms of these integrals, we can rewrite the relations (76) and (77) in the form

$$A = \frac{M}{2\pi I_{\gamma,0}(x)}, \quad (81)$$

and

$$b \equiv \frac{2\pi B}{kM} = \frac{I_{\gamma,1}(x)}{I_{\gamma,0}(x)}. \quad (82)$$

Combining Eqs. (69), (81) and (82) and introducing the normalized polytropic temperature [9]:

$$\eta \equiv (2\pi)^{\gamma-1}\frac{kM^{2-\gamma}}{4\pi K}, \quad (83)$$

we find that

$$\eta = \frac{x}{2}\frac{I_{\gamma,0}(x)^{2-\gamma}}{I_{\gamma,1}(x)}. \quad (84)$$

Equations (82) and (84) determine the magnetization B as a function of the polytropic temperature K in a parametric form (with parameter x). For $\gamma \to 1$, we recover the self-consistency relation (26) of [9]. Some curves are plotted in Fig. 2 for $n \geq 1/2$. The case of negative indices $n < -1$ is very similar to the isothermal case [9] and will not be illustrated in detail. For $x \to x_*$, $b \to 1$, $\eta \to +\infty$ and $\epsilon \to -2$.

4.4 The energy

4.4.1 The homogeneous phase

In the homogeneous phase, the density is uniform with value $\rho = M/(2\pi)$ and the magnetization vanishes ($B =$

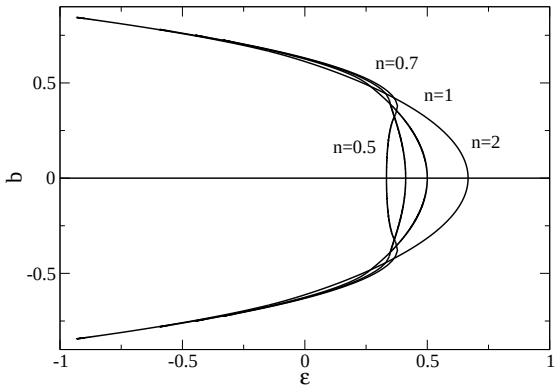

Fig. 3. Magnetization as a function of the energy for $n \geq 1/2$.

0). Therefore, the energy (64) reduces to the kinetic energy

$$E = \frac{1}{2}\int_0^{2\pi} p\, d\theta = \frac{1}{2}K\int_0^{2\pi} \rho^\gamma\, d\theta = K\pi\left(\frac{M}{2\pi}\right)^\gamma. \quad (85)$$

Introducing the dimensionless energy [9]:

$$\epsilon \equiv \frac{8\pi E}{kM^2}, \quad (86)$$

and recalling the expression (83) of the dimensionless polytropic temperature, we find that the caloric curve[18] for the homogeneous distribution is simply [9]:

$$\eta = \frac{1}{\epsilon}. \quad (87)$$

It has been shown in [9,48] that the homogeneous phase is stable iff

$$\eta \leq \eta_c = \gamma, \qquad \epsilon \geq \epsilon_c = \frac{1}{\gamma}. \quad (88)$$

4.4.2 The inhomogeneous phase

To compute the kinetic energy in the inhomogeneous phase, without introducing new integrals, we shall use a trick inspired from the astrophysical problem [46]. The condition of equilibrium can be written as a condition of hydrostatic balance (see Appendix A) [9]:

$$\frac{dp}{d\theta} = -\rho\frac{d\Phi}{d\theta}. \quad (89)$$

For a polytropic equation of state, we have

$$p = K\rho^\gamma. \quad (90)$$

Therefore, the foregoing equation can be integrated into

$$\Phi = -\frac{K\gamma}{\gamma-1}\rho^{\gamma-1} + C. \quad (91)$$

[18] We shall explain in Sec. 5 why this is the relevant caloric curve to consider.

We must be careful that this relation is valid only in the region where $\rho > 0$. We must therefore consider two cases. For incomplete polytropes, using $\Phi(\pi) = B$, we get

$$\Phi = -\frac{K\gamma}{\gamma-1}(\rho^{\gamma-1} - \rho(\pi)^{\gamma-1}) + B. \quad (92)$$

On the other hand, for complete polytropes, using $\rho(\theta_c) = 0$ and $\Phi(\theta_c) = -B\cos\theta_c$, we get

$$\Phi = -\frac{K\gamma}{\gamma-1}\rho^{\gamma-1} - B\cos\theta_c. \quad (93)$$

These two cases can be combined in a single formula

$$\Phi = -\frac{K\gamma}{\gamma-1}(\rho^{\gamma-1} - \rho(\pi)^{\gamma-1}) - B\cos\theta_c. \quad (94)$$

For incomplete polytropes $\theta_c = \pi$, and for complete polytropes $\rho(\pi) = 0$. Substituting Eq. (94) in the potential energy (58) and using Eq. (90), we obtain

$$W = -\frac{1}{2}\frac{\gamma}{\gamma-1}\int p\, d\theta + \frac{1}{2}\frac{K\gamma}{\gamma-1}M\rho(\pi)^{\gamma-1} - \frac{1}{2}MB\cos\theta_c. \quad (95)$$

In the first integral, we recognize the kinetic energy (64). Therefore, we obtain

$$E_{kin} = -\frac{\gamma-1}{\gamma}W + \frac{1}{2}KM\rho(\pi)^{\gamma-1} - \frac{1}{2}\frac{\gamma-1}{\gamma}MB\cos\theta_c. \quad (96)$$

Using the expression (64) of the potential energy, we get

$$E_{kin} = \frac{\gamma-1}{\gamma}\frac{\pi B^2}{k} - \frac{1}{2}\frac{\gamma-1}{\gamma}MB\cos\theta_c + \frac{1}{2}KM\rho(\pi)^{\gamma-1}. \quad (97)$$

Finally, the total energy $E = E_{kin} + W$ is

$$E = -\frac{\pi B^2}{\gamma k} - \frac{1}{2}\frac{\gamma-1}{\gamma}MB\cos\theta_c + \frac{1}{2}KM\rho(\pi)^{\gamma-1}. \quad (98)$$

Using Eqs. (82) and (68), the normalized energy (86) can be written

$$\epsilon = -\frac{2}{\gamma}b^2 - 2\frac{\gamma-1}{\gamma}b\cos\theta_c + 2\frac{b}{x}\left(1 - \frac{\gamma-1}{\gamma}x\right)_+. \quad (99)$$

Using Eq. (82), it can also be written explicitly in terms of x as

$$\epsilon = -\frac{2}{\gamma}\frac{I_{\gamma,1}(x)^2}{I_{\gamma,0}(x)^2} - 2\frac{\gamma-1}{\gamma}\frac{I_{\gamma,1}(x)}{I_{\gamma,0}(x)}\cos\theta_c + \frac{2}{x}\frac{I_{\gamma,1}(x)}{I_{\gamma,0}(x)}\left(1 - \frac{\gamma-1}{\gamma}x\right)_+. \quad (100)$$

Equations (82) and (100) determine the magnetization b as a function of the energy ϵ in a parametric form. Some curves are plotted in Fig. 3 for $n \geq 1/2$. On the other hand, the caloric curve $\eta(\epsilon)$ is determined by Eqs. (84) and (100). Some curves are plotted in Fig. 4 for $n \geq 1/2$ and in Fig. 5 for $n < -1$. They complete Fig. 12 of [9] by adding the inhomogeneous branches. They will be analyzed in Sec. 5.

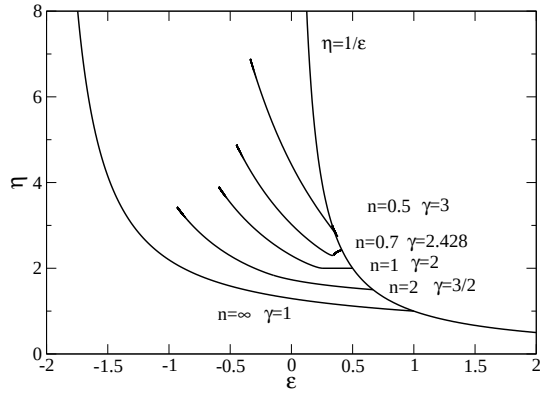

Fig. 4. Caloric curve for polytropes with positive indices $n \geq 1/2$.

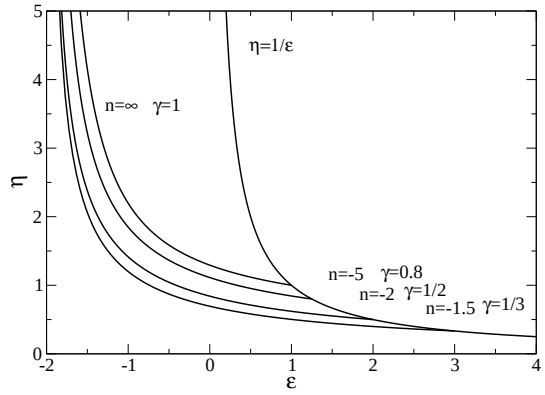

Fig. 5. Caloric curve for polytropes with negative indices $n < -1$.

4.5 The averaged kinetic temperature

The local kinetic temperature is defined by

$$T_{kin}(\theta) = \langle v^2 \rangle(\theta) = \frac{\int f v^2 \, dv}{\int f \, dv}. \tag{101}$$

The averaged kinetic temperature is therefore

$$\langle T_{kin} \rangle = \frac{1}{M} \int_0^{2\pi} \rho(\theta) \langle v^2 \rangle(\theta) \, d\theta = \frac{2E_{kin}}{M}. \tag{102}$$

Defining the normalized kinetic energy and the normalized averaged kinetic temperature by

$$\epsilon_{kin} = \frac{8\pi E_{kin}}{kM^2}, \qquad \Theta = \frac{4\pi \langle T_{kin} \rangle}{kM}, \tag{103}$$

we obtain

$$\Theta = \epsilon_{kin}. \tag{104}$$

If we define the normalized potential energy by

$$w = \frac{8\pi W}{kM^2}, \tag{105}$$

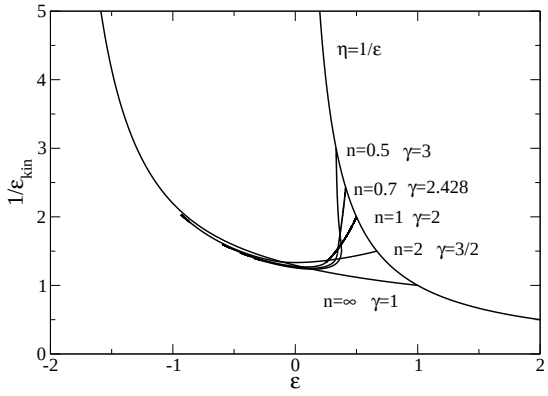

Fig. 6. Inverse averaged kinetic temperature as a function of the energy for polytropes with positive indices $n \geq 1/2$.

and use Eqs. (64) and (82), we obtain

$$w = -2b^2. \tag{106}$$

Finally, the total energy $E = E_{kin} + W$ can be written in dimensionless form

$$\epsilon = \epsilon_{kin} + w = \epsilon_{kin} - 2b^2. \tag{107}$$

From Eqs. (99) and (107), we obtain

$$\epsilon_{kin} = \Theta = 2\frac{\gamma - 1}{\gamma} b^2 - 2\frac{\gamma - 1}{\gamma} b \cos\theta_c + 2\frac{b}{x}\left(1 - \frac{\gamma - 1}{\gamma} x\right)_+. \tag{108}$$

Using Eq. (82), this can also be written explicitly in terms of x as

$$\epsilon_{kin} = \Theta = 2\frac{\gamma - 1}{\gamma}\frac{I_{\gamma,1}(x)^2}{I_{\gamma,0}(x)^2} - 2\frac{\gamma - 1}{\gamma}\frac{I_{\gamma,1}(x)}{I_{\gamma,0}(x)} \cos\theta_c + \frac{2}{x}\frac{I_{\gamma,1}(x)}{I_{\gamma,0}(x)}\left(1 - \frac{\gamma - 1}{\gamma} x\right)_+. \tag{109}$$

Equations (109) and (100) determine the physical caloric curve $\epsilon_{kin}(\epsilon)$ or $\Theta(\epsilon)$ in a parametric form. Some curves are represented in Fig. 6 for $n \geq 1/2$. In the homogeneous phase, we have

$$\epsilon = \epsilon_{kin} = \Theta. \tag{110}$$

These physical caloric curves will be analyzed in Sec. 6.

4.6 The free energy

According to Eq. (53), the free energy of the polytropes can be written in terms of the density as

$$F = \frac{1}{2} \int \rho \Phi \, d\theta + \frac{K}{\gamma - 1} \int \rho^\gamma \, d\theta, \tag{111}$$

up to an unimportant constant. In the second term, we recognize the kinetic energy (64) while the first term is just the potential energy, so that

$$F = W + \frac{2}{\gamma - 1} E_{kin}. \tag{112}$$

Introducing the normalized free energy

$$f = \frac{8\pi F}{kM^2}, \tag{113}$$

we obtain

$$f = w + \frac{2}{\gamma - 1} \epsilon_{kin}. \tag{114}$$

Substituting Eqs. (106) and (108) in Eq. (114), we find that

$$f = \frac{2(2-\gamma)}{\gamma} b^2 - \frac{4}{\gamma} b \cos\theta_c + \frac{4}{\gamma - 1} \frac{b}{x} \left(1 - \frac{\gamma - 1}{\gamma} x\right)_+. \tag{115}$$

Using Eq. (82), this can be explicitly written in terms of x as

$$f = \frac{2(2-\gamma)}{\gamma} \frac{I_{\gamma,1}(x)^2}{I_{\gamma,0}(x)^2} - \frac{4}{\gamma} \frac{I_{\gamma,1}(x)}{I_{\gamma,0}(x)} \cos\theta_c + \frac{1}{\gamma - 1} \frac{4}{x} \frac{I_{\gamma,1}(x)}{I_{\gamma,0}(x)} \left(1 - \frac{\gamma - 1}{\gamma} x\right)_+. \tag{116}$$

Equations (116) and (84) determine the free energy as a function of the polytropic temperature $f(\eta)$ in a parametric form. Some curves are represented in Figs. 7 and 8 for $n \geq 1/2$. They will be analyzed in Sec. 5. In the homogeneous phase, Eq. (112) reduces to $F = 2E/(\gamma - 1)$. Using Eq. (87), we get

$$f = \frac{2}{\gamma - 1} \frac{1}{\eta}. \tag{117}$$

4.7 The entropy

According to Eq. (51), the entropy of the polytropes can be written in terms of the density as

$$S = -\left(n - \frac{1}{2}\right) \beta \int p \, d\theta, \tag{118}$$

up to an unimportant constant. In the second term, we recognize the kinetic energy (64) so that

$$S = -2\left(n - \frac{1}{2}\right) \beta E_{kin}. \tag{119}$$

On the other hand, the inverse thermodynamical temperature $\beta = 1/T$ is related to the polytropic temperature K by Eq. (30). Therefore, the entropy can be rewritten

$$S = -\left(n - \frac{1}{2}\right) \frac{2E_{kin}}{C_n K^{\frac{2n}{2n-1}}}. \tag{120}$$

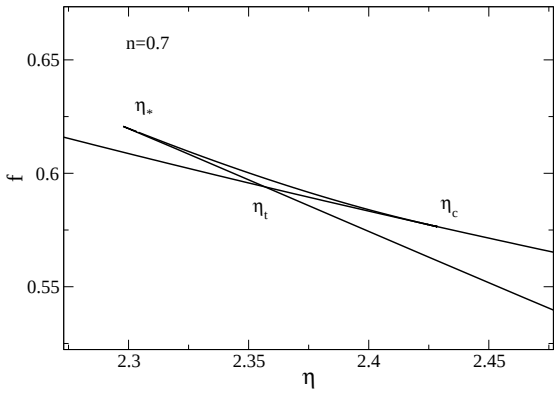

Fig. 7. Free energy as a function of the inverse polytropic temperature for $n = 0.7$. It exhibits a first order canonical phase transition marked by the discontinuity of $df/d\eta$ at $\eta = \eta_t$.

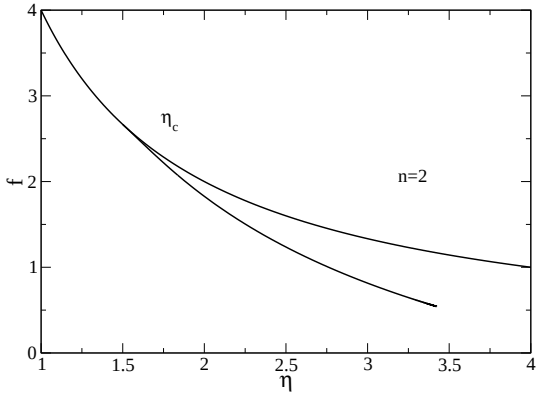

Fig. 8. Free energy as a function of the inverse polytropic temperature for $n = 2$. It exhibits a second order phase transition marked by the discontinuity of $d^2f/d\eta^2$ at $\eta = \eta_c$.

Defining the normalized entropy by

$$s = \frac{C_n (\pi k)^{\frac{1}{2n-1}}}{M^{\frac{2n}{2n-1}}} S, \tag{121}$$

we obtain

$$s = -\left(n - \frac{1}{2}\right) \epsilon_{kin} \eta^{\frac{2n}{2n-1}}. \tag{122}$$

Using Eqs. (84) and (108), this gives s as a function of x. Finally, Eqs. (122) and (100) determine the entropy as a function of the energy $s(\epsilon)$ in a parametric form. Some curves are represented in Figs. 9 and 10 for $n \geq 1/2$. They will be analyzed in Sec. 5. For the homogeneous phase, using $\epsilon = \epsilon_{kin}$ and $\eta = 1/\epsilon$, we get

$$s = -\left(n - \frac{1}{2}\right) \frac{1}{\epsilon^{\frac{1}{2n-1}}}. \tag{123}$$

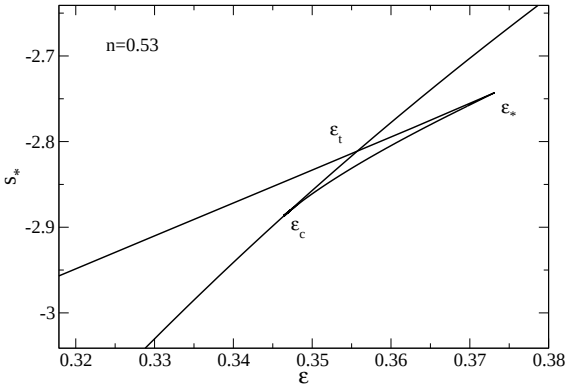

Fig. 9. Entropy as a function of energy for $n = 0.53$. It exhibits a microcanonical first order phase transition marked by the discontinuity of $ds/d\epsilon$ at $\epsilon = \epsilon_t$. To avoid the occurrence of large numbers when $n \simeq 0.5$, we have plotted $s_* = -\epsilon_{kin}^{2n-1}\eta^{2n}$ and $s_*^{homo} = -1/\epsilon$ as a function of ϵ.

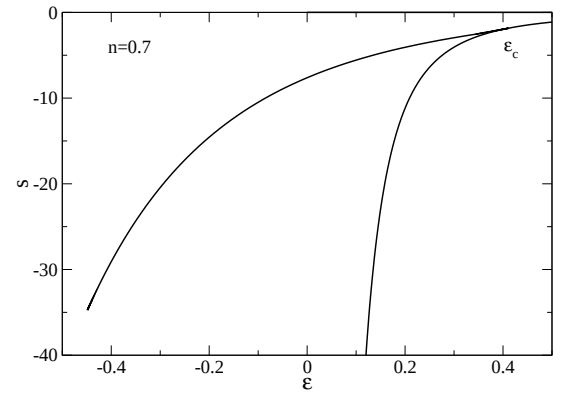

Fig. 10. Entropy as a function of energy for $n = 0.7$. It exhibits a microcanonical second order phase transition marked by the discontinuity of $d^2s/d\epsilon^2$ at $\epsilon = \epsilon_c$. There is also a small convex dip (hardly visible) evidencing a region of negative specific heats and a canonical first order phase transition.

5 The thermodynamical caloric curve

5.1 General comments

Basically, we want to study the optimization problems (4) and (5) where S is the Tsallis entropy (11). The maximization problem (4) corresponds to a condition of microcanonical stability and the minimization problem (5) to a condition of canonical stability[19]. It is well-known that the two optimization problems (4) and (5) have the same critical points canceling the first order variations of the thermodynamical potential. The critical points of the maximization problem (4) are given by Eq. (16) where β and α are Lagrange multipliers associated with the constraints E and M. Here, $\beta = 1/T$ represents the inverse thermodynamical temperature. It satisfies the thermodynamical relation $\beta = (\partial S/\partial E)_M$. For the Tsallis entropy, the critical points in the microcanonical ensemble are given by Eq. (17). The critical points of the minimization problem (5) are given by $\delta F + \alpha T\delta M = 0$ where α is a Lagrange multiplier associated with the constraint M. Obviously, these first order variations are equivalent to Eq. (16) so that the critical points in the canonical ensemble are again given by Eq. (17). Although the critical points are the same, their stability can differ in the microcanonical and canonical ensembles. From general theorems [50], we know that a critical point is stable in the microcanonical ensemble (maximum of S at fixed E and M) if it is stable in the canonical ensemble (minimum of F at fixed M) but the reciprocal may be wrong. In that case, we have ensembles inequivalence. Related to this property, we can show that the thermodynamical specific heat $C = dE/dT$ is always positive in the canonical ensemble while is can be positive or negative in the microcanonical ensemble. These are general results valid for all entropies of the form (3), including the Tsallis entropy (11), provided that we use the proper thermodynamical variable E and $\beta = (\partial S/\partial E)_M$ that are canonically conjugate with respect to the entropy S. Therefore, the proper thermodynamical caloric curve associated with the optimization problems (4) and (5) is the one giving the inverse temperature $\beta = 1/T$ (Lagrange multiplier) as a function of the energy E. It is from this curve that we can study ensembles inequivalence [50]. It is also from this curve that we can apply the Poincaré theory on the linear series of equilibria [59,60]. Now, for polytropic distributions, we have seen in Eq. (30) that the polytropic temperature K is always a monotonic function of the thermodynamical temperature T. Therefore, for convenience, we can equivalently consider the caloric curve giving the polytropic temperature K as a function of the energy E (the preceding properties are unchanged). This is the choice that has been made in the gravitational problem [46,39] and that we shall make here. Therefore, we shall call $K(E)$ the thermodynamical caloric curve. In dimensionless variables, it corresponds to $\eta(\epsilon)$. Several caloric curves $\eta(\epsilon)$ have been plotted in Figs. 4 and 5 for different indices n. In order to understand their behavior let us first consider the asymptotic limits $x \to 0$ and $x \to +\infty$.

5.2 The limit $x \to 0$

For $x \to 0$, the deformed Bessel functions (78) can be approximated by

$$I_{\gamma,0}(x) = 1 + \frac{2-\gamma}{4\gamma^2}x^2 + ..., \qquad (124)$$

$$I_{\gamma,1}(x) = \frac{x}{2\gamma} + \frac{(\gamma-2)(2\gamma-3)}{16\gamma^3}x^3 + ... \qquad (125)$$

[19] Recall that these optimization problems can be given a dynamical interpretation (see Sec. 2.2). For convenience, we use here a thermodynamical language based on the *thermodynamical analogy* described in Sec. 2.2. We should add the prefix "pseudo" (i.e. pseudo entropy, pseudo temperature...) but for simplicity, we avoid it.

Then, we obtain the expansions

$$b = \frac{x}{2\gamma} + \frac{(\gamma-2)(2\gamma-1)}{16\gamma^3}x^3 + ... \quad (126)$$

$$\eta = \gamma + \frac{2-\gamma}{8\gamma}x^2 + ..., \quad (127)$$

$$\epsilon = \frac{1}{\gamma} + (2\gamma^2 - 5\gamma - 2)\frac{x^2}{8\gamma^3} + ... \quad (128)$$

$$\epsilon_{kin} = \Theta = \frac{1}{\gamma} + (2\gamma^2 - \gamma - 2)\frac{x^2}{8\gamma^3} + ... \quad (129)$$

From these expressions, we can draw the following conclusions. Let us introduce the critical indices

$$\gamma_* = \frac{5+\sqrt{41}}{4} \simeq 2.8507811... \quad (130)$$

$$n_* = \frac{4}{1+\sqrt{41}} \simeq 0.54031242... \quad (131)$$

Let us first consider the case $n \geq 1/2$ so that $1 \leq \gamma \leq 3$. The quantity $2\gamma^2 - 5\gamma - 2$ is positive for $\gamma_* < \gamma \leq 3$, i.e. $1/2 \leq n < n_*$, showing that the energy increases as x increases. The quantity $2\gamma^2 - 5\gamma - 2$ is negative for $1 \leq \gamma < \gamma_*$, i.e. $n > n_*$. In that case, the energy decreases as x increases. On the other hand, for $2 < \gamma \leq 3$, i.e. $1/2 \leq n < 1$, the inverse temperature η decreases as x increases. By contrast, for $1 \leq \gamma < 2$, i.e. $n > 1$, the inverse temperature η increases as x increases. This explains the behavior of the caloric curve $\eta(\epsilon)$ close to the bifurcation point. Close to that point, we have

$$\eta - \eta_c = \frac{(2-\gamma)\gamma^2}{2\gamma^2 - 5\gamma - 2}(\epsilon - \epsilon_c) + ... \quad (132)$$

The specific heat is

$$C_T = \frac{dE}{dT} = -\beta^2\frac{dE}{d\beta}. \quad (133)$$

Since T is a monotonically increasing function of K, we can equivalently consider the quantity

$$C_K = -\eta^2\frac{d\epsilon}{d\eta}. \quad (134)$$

At the bifurcation point, we have

$$C_K = -\frac{2\gamma^2 - 5\gamma - 2}{2-\gamma}. \quad (135)$$

The specific heat close to the bifurcation point is positive for $1/2 \leq n < n_*$, negative for $n_* < n < 1$ and positive again for $n > 1$. It vanishes for $n = n_*$ and it is infinite for $n = 1$. Let us now consider the case $n < -1$ so that $0 < \gamma \leq 1$. In that case, η increases as x increases. On the other hand, the quantity $2\gamma^2 - 5\gamma - 2$ is always negative so that ϵ decreases as x increases. Therefore, the specific heat is always positive.

5.3 The limit $x \to +\infty$

Let us first consider $n \geq 1/2$. For $x \to +\infty$, we find that $\theta_c \to \frac{\pi}{2}$. The deformed Bessel functions can be approximated by

$$I_{\gamma,0}(x) \sim \frac{1}{2\pi}\frac{1}{(n+1)^n}x^n\sqrt{\pi}\frac{\Gamma\left(\frac{1+n}{2}\right)}{\Gamma\left(\frac{2+n}{2}\right)}, \quad (136)$$

$$I_{\gamma,1}(x) \sim \frac{1}{2\pi}\frac{1}{(n+1)^n}x^n\sqrt{\pi}\frac{\Gamma\left(\frac{2+n}{2}\right)}{\Gamma\left(\frac{3+n}{2}\right)}. \quad (137)$$

The normalization constant (81) behaves like

$$A \sim M(n+1)^n\frac{1}{x^n}\frac{1}{\sqrt{\pi}}\frac{\Gamma\left(\frac{2+n}{2}\right)}{\Gamma\left(\frac{1+n}{2}\right)}, \quad (138)$$

and the density profile (68) tends to the limit distribution

$$\rho(\theta) = \frac{M}{\sqrt{\pi}}\frac{\Gamma\left(\frac{2+n}{2}\right)}{\Gamma\left(\frac{1+n}{2}\right)}\cos^n\theta. \quad (139)$$

Finally, the thermodynamical parameters tend to the limit values:

$$\eta \to \eta_\infty \equiv \frac{1}{2}(2\pi)^{1/n}\frac{n+1}{(\sqrt{\pi})^{1/n}}\frac{\Gamma\left(\frac{1+n}{2}\right)^{\frac{n-1}{n}}\Gamma\left(\frac{3+n}{2}\right)}{\Gamma\left(\frac{2+n}{2}\right)^{\frac{2n-1}{n}}}, \quad (140)$$

$$b \to \frac{\Gamma\left(\frac{2+n}{2}\right)^2}{\Gamma\left(\frac{3+n}{2}\right)\Gamma\left(\frac{1+n}{2}\right)}, \quad (141)$$

$$\epsilon \to \epsilon_\infty \equiv -\frac{2n}{n+1}\frac{\Gamma\left(\frac{2+n}{2}\right)^4}{\Gamma\left(\frac{3+n}{2}\right)^2\Gamma\left(\frac{1+n}{2}\right)^2}, \quad (142)$$

$$\epsilon_{kin} = \Theta \to \frac{2}{n+1}\frac{\Gamma\left(\frac{2+n}{2}\right)^4}{\Gamma\left(\frac{3+n}{2}\right)^2\Gamma\left(\frac{1+n}{2}\right)^2}. \quad (143)$$

This implies in particular that the polytropes $n \geq 1/2$ only exist for $\epsilon \geq \epsilon_\infty$ and $\eta \leq \eta_\infty$. Beyond these points, there is no polytropic distribution anymore. In that case, the system is likely to converge towards the Lynden-Bell distribution (see Sec. 7.2).

5.4 Phase transitions

We are now in a position to describe in detail the phase transitions that occur in the thermodynamical caloric curve $K(E)$ or, in dimensionless form $\eta(\epsilon)$, plotted in Figs. 4 and 5. Note that this curve represents the full series of equilibria containing all critical points of entropy or free energy. We now have to determine which solutions correspond to fully stable (S) solutions (global maxima of S in MCE or global minima of F in CE), metastable (M) solutions (local maxima of S in MCE or local minima of F in CE) or unstable (U) solutions (saddle points of S or

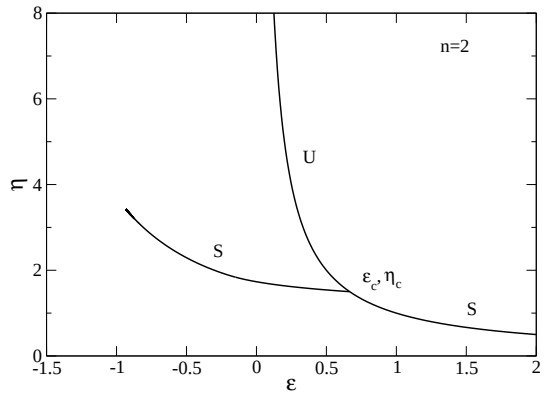

Fig. 11. For $n > n_{CTP} = 1$ (specifically $n = 2$), the caloric curve exhibits second order canonical and microcanonical phase transitions. The ensembles are equivalent.

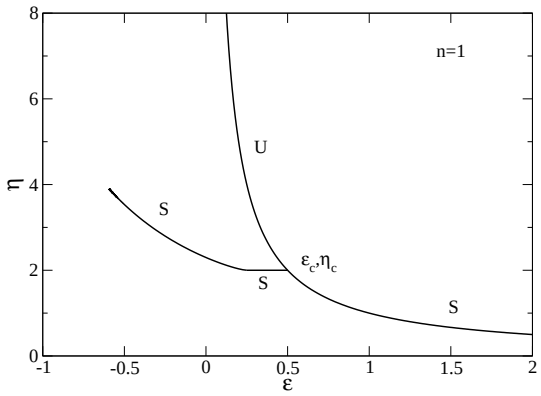

Fig. 12. For $n = n_{CTP} = 1$, there is a degeneracy in the canonical ensemble for $\eta = \eta_c = 2$. In the microcanonical ensemble, there is a region of infinite specific heats.

F). To make this selection, we can compare the equilibrium entropy or free energy of the solutions in competition (see Secs. 4.6 and 4.7) or use the Poincaré theory of linear series of equilibria [59,60].

Let us first consider the canonical ensemble (CE) where the control parameter is the inverse polytropic temperature η. For $n > n_{CTP} = 1$, the caloric curve $\epsilon(\eta)$ exhibits a second order phase transition (see Figs. 4, 8 and 11) marked by the discontinuity of $d\epsilon/d\eta$ at $\eta = \eta_c$. The homogeneous solution is fully stable for $\eta < \eta_c$ and it becomes unstable for $\eta > \eta_c$. At that point it is replaced by the inhomogeneous branch that is fully stable. The series of equilibria presents one solution for $\eta < \eta_c$ (the solution $b = 0$ that is fully stable) and three solutions for $\eta > \eta_c$ (two solutions $\pm b \neq 0$ that are fully stable and one solution $b = 0$ that is unstable); see Fig. 2. For $n = n_{CTP} = 1$, there is a degeneracy[20] at $\eta = \eta_c = 2$ since there exists an infinity of solutions $-1/2 \leq b \leq 1/2$ with the same free energy (see Figs. 2, 4 and 12). For $1/2 \leq n < n_{CTP} = 1$, the caloric curve $\epsilon(\eta)$ exhibits a first order phase transition between the homogeneous and inhomogeneous phases (see Figs. 4, 7 and 13) marked by the discontinuity of ϵ at $\eta = \eta_t$ and the existence of metastable branches. The series of equilibria presents one solution for $\eta < \eta_*$ (the solution $b = 0$ that is fully stable), five solutions for $\eta_* < \eta < \eta_c$ (two solutions $\pm b \neq 0$ that are fully stable or metastable, two solutions $\pm b' \neq 0$ that are unstable and one solution $b = 0$ that is fully stable or metastable) and three solutions for $\eta > \eta_c$ (two solutions $\pm b \neq 0$ that are fully stable and one solution $b = 0$ that is unstable); see Fig. 2. Therefore, $n_{CTP} = 1$ and $\eta_c = 2$ (corresponding to $\epsilon_c = 1/2$) is a canonical tricritical point separating first and second order phase transitions. The canonical phase diagram in the (n, η) plane is represented in Fig. 14.

Let us now consider the microcanonical ensemble (MCE) where the control parameter is the energy ϵ. For $n > n_{MCP} \simeq 0.68$, the caloric curve $\eta(\epsilon)$ exhibits a second order phase transition marked by the discontinuity of

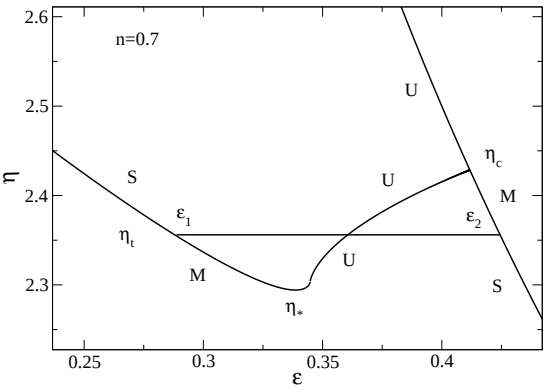

Fig. 13. Caloric curve in the canonical ensemble for $0.5 \leq n < n_{CTP} = 1$ (specifically $n = 0.7$). It exhibits a canonical first order phase transition marked by the discontinuity of ϵ at $\eta = \eta_t$. The temperature of transition can be obtained by comparing the free energy of the homogeneous and inhomogeneous phases (see Fig. 7). The Maxwell construction does not directly apply in the present situation since we have used $1/K$ instead of β in the caloric curve. The stability of the solutions (denoted S, M, and U) can be settled by using the Poincaré theorem [59,60]. The temperatures η_* and η_c are spinodal points marking the end of the metastable branches.

$d\eta/d\epsilon$ at $\epsilon = \epsilon_c$ (see Figs. 4, 10, 11, 12 and 15). The homogeneous solution is fully stable for $\epsilon > \epsilon_c$ and it becomes unstable for $\epsilon < \epsilon_c$. At that point it is replaced by the inhomogeneous branch that is fully stable. For $n > n_{CTP} = 1$, the specific heat is positive and the ensembles are equivalent (see Fig. 11). For $n_{MCP} < n < n_{CTP} = 1$, there is a region of negative specific heat in the microcanonical ensemble between ϵ' and ϵ_c (see Fig. 15) that is replaced by a phase transition in the canonical ensemble (see Fig. 13). The series of equilibria presents one solution for $\epsilon > \epsilon_c$ (the solution $b = 0$ that is fully stable) and three solutions for $\epsilon < \epsilon_c$ (two solutions $\pm b \neq 0$ that are fully stable and one solution $b = 0$ that is unstable); see Fig. 3. The corresponding microcanonical phase diagram in the (n, ϵ) plane is represented in Fig. 16. For

[20] This is a bit similar to critical polytropes $n_c = 3$ in astrophysics [61].

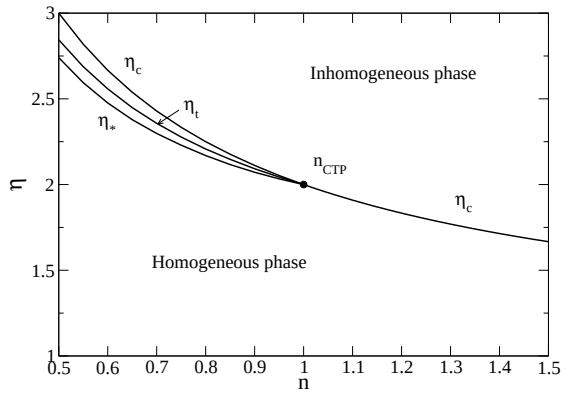

Fig. 14. Phase diagram in the canonical ensemble. There is a canonical tricritical point located at $n_{CTP}=1$ and $\eta=2$ separating first and second order phase transitions.

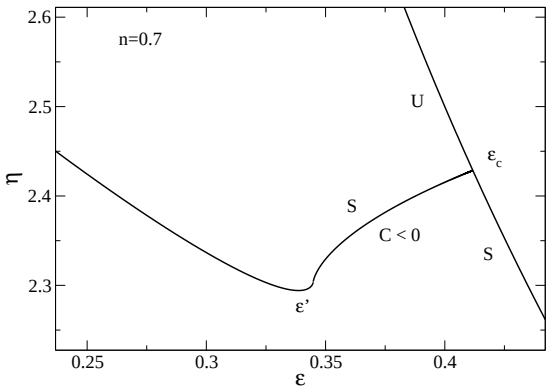

Fig. 15. Caloric curve in the microcanonical ensemble for $n_{MCP}<n<n_{CTP}=1$ (specifically $n=0.7$). The inhomogeneous states are fully stable. There is a region of negative specific heats between ϵ' et ϵ_c. In the canonical ensemble, this region is replaced by a phase transition.

$n_{MTP}\simeq 0.563<n<n_{MCP}\simeq 0.68$, there is a very interesting situation[21] in which the caloric curve exhibits a second order phase transition at ϵ_c between the homogeneous phase and the inhomogeneous phase (as before) and a first order phase transition at ϵ_t between two inhomogeneous phases (see Fig. 17). The first order phase transition is marked by the discontinuity of η at $\epsilon=\epsilon_t$ and the existence of metastable branches. For $n=0.6$, the series of equilibria presents one solution for $\epsilon>\epsilon_c$ (the solution $b=0$ that is fully stable), three solutions for $\epsilon_*<\epsilon<\epsilon_c$ (two solutions $\pm b\neq 0$ that are fully stable and one solution $b=0$ that is unstable), seven solutions for $\epsilon'_*<\epsilon<\epsilon_*$ (four solutions $\pm b\neq 0$ and $\pm b''\neq 0$ that are fully stable or metastable, two solutions $\pm b'\neq 0$ that are unstable and one solution $b=0$ that is unstable) and three solutions for $\epsilon<\epsilon'_*$ (two solutions $\pm b\neq 0$ that are fully stable and one solution $b=0$ that is unstable). Therefore, $n_{MCP}\simeq 0.68$ and $\epsilon\simeq 0.3492$ (corresponding to $\eta=2.336$) is a microcanonical critical point marking the appearance of the first order phase transition. At $n=n_{MTP}\simeq 0.563$, the energies of the first and second order phase transitions coincide ($\epsilon_t=\epsilon_c$) and, for $1/2\leq n<n_{MTP}\simeq 0.563$, there is only a first order phase transition at $\epsilon=\epsilon_t$ between homogeneous and inhomogeneous states. Therefore, $n_{MTP}\simeq 0.563$ and $\epsilon\simeq 0.3603$ (corresponding to $\eta=2.776$) is a microcanonical tricritical point separating first and second order phase transitions. For $n_*\simeq 0.54<n<n_{MTP}\simeq 0.563$, there remains a sort of second order phase transition at $\epsilon=\epsilon_c$ for the *metastable* states (see Fig. 18). Between ϵ'_* and ϵ_c, the specific heat is negative. For $n=n_*\simeq 0.54$, the energies ϵ'_* and ϵ_c coincide and for $1/2\leq n<n_*$, the "metastable" second order phase transition disappears. In that case, there is only a first order phase transition (see Figs. 9 and 19). The series of equilibria presents one solution for $\epsilon>\epsilon_*$ (the solution $b=0$ that is fully stable), five solutions for $\epsilon_c<\epsilon<\epsilon_*$ (two solutions $\pm b\neq 0$ that are fully stable or metastable, two solutions $\pm b'\neq 0$ that are unstable and one solution $b=0$ that is fully stable or metastable) and three solutions for $\epsilon<\epsilon_c$ (two solutions $\pm b\neq 0$ that

[21] To our knowledge, this is the first example of that kind.

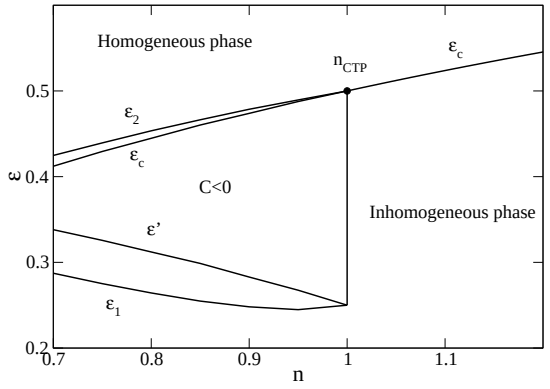

Fig. 16. Phase diagram in the microcanonical ensemble. In this range of indices, there is only a second order phase transition at energy ϵ_c. The states between ϵ' et ϵ_c have negative specific heats. They are inaccessible in the canonical ensemble (saddle points of free energy). If we consider only fully stable states, the ensembles are inequivalent between ϵ_1 and ϵ_2 (see Fig. 13). If we take into account canonical metastable states, the ensembles are inequivalent between ϵ' and ϵ_c.

are fully stable and one solution $b=0$ that is unstable); see Fig. 3. The microcanonical phase diagram in the (n,ϵ) plane, summarizing all these results, is represented in Fig. 20.

In conclusion, for $1/2\leq n<n_{MTP}$, we have canonical and microcanonical first order phase transitions, for $n_{MTP}<n<n_{MCP}$, we have canonical first order transitions, microcanonical first order transitions and microcanonical second order transitions, for $n_{MCP}<n<n_{CTP}=1$, we have canonical first order phase transitions and microcanonical second order phase transitions and for $n>n_{CTP}=1$, we have canonical and microcanonical second order phase transitions. The ensembles are equivalent for $n>n_{CTP}=1$ and inequivalent for $n<n_{CTP}=1$ in some range of energies. The microcanonical and canonical tricritical points do not coincide. Similar observations

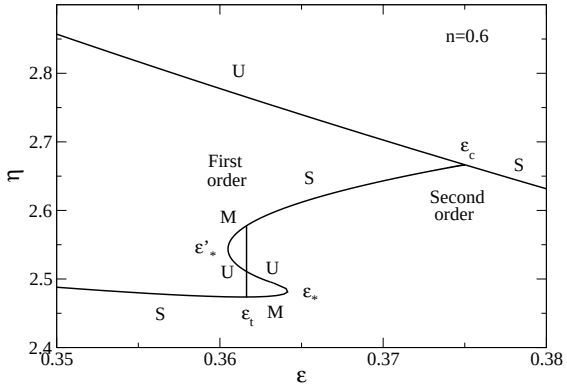

Fig. 17. Caloric curve in the microcanonical ensemble for $n_{MTP} < n < n_{MCP}$ (specifically $n = 0.6$). Interestingly, there exists microcanonical second order *and* first order phase transitions on the same curve. The second order phase transition is marked by the discontinuity of $d\eta/d\epsilon$ at $\epsilon = \epsilon_c$. The first order phase transition marked by the discontinuity of η at $\epsilon = \epsilon_t$. The stability of the solutions (denoted S, M, and U) can be settled by using the Poincaré theorem [59,60]. The energies ϵ'_* and ϵ_* are spinodal points marking the end of the metastable branches.

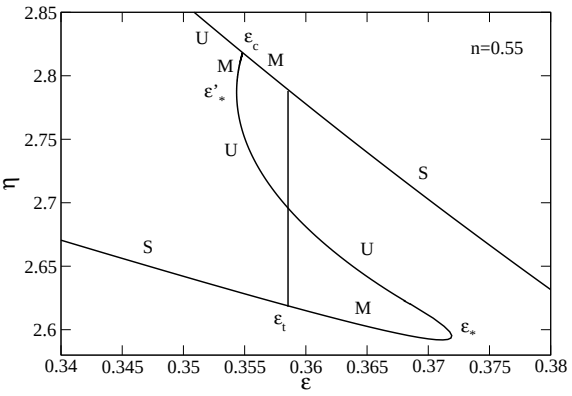

Fig. 18. Caloric curve in the microcanonical ensemble for $n_* < n < n_{MTP}$ (specifically $n = 0.55$). If we only consider fully stable states, there is only a first order phase transition at $\epsilon = \epsilon_t$. If we consider the metastable states, there is a second order phase transition at $\epsilon = \epsilon_c$. The spinodal points marking the end of the metastable branches are ϵ'_* and ϵ_*.

have been made for other models [62-65]. For $n < -1$, we have canonical and microcanonical second order phase transitions and the ensembles are equivalent.

Using the thermodynamical analogy of Sec. 2.2, we conclude that the polytropes denoted (S) or (M) that are maxima of pseudo entropy S at fixed mass and energy are nonlinearly dynamically stable according to the "microcanonical" criterion (4). We cannot conclude that the polytropes denoted (U) are dynamically unstable since (4) provides just a sufficient condition of nonlinear dynamical stability.

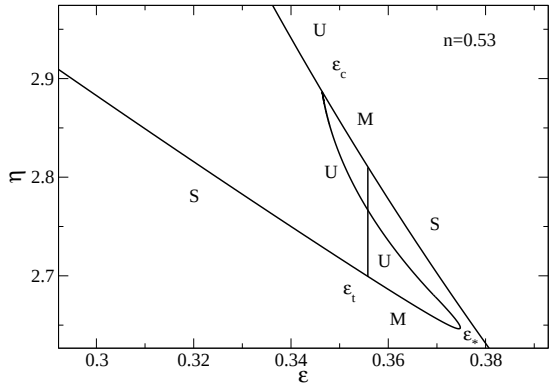

Fig. 19. Caloric curve in the microcanonical ensemble for $1/2 \leq n < n_*$ (specifically $n = 0.53$). There is only a first order phase transition at $\epsilon = \epsilon_t$. The spinodal points marking the end of the metastable branches are ϵ_c and ϵ_*. Note that there exists a small region of negative specific heats between the turning points of energy and temperature that is metastable.

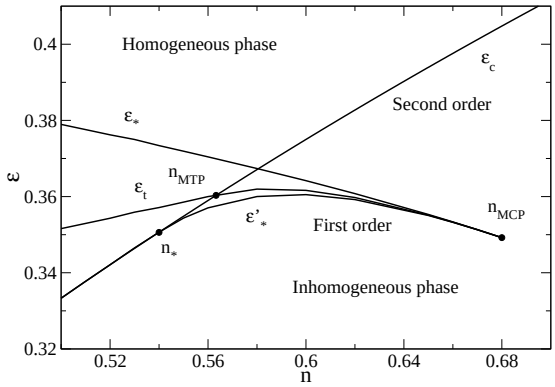

Fig. 20. Phase diagram in the microcanonical ensemble. For $n > n_{MCP}$ ($n_{MCP} \simeq 0.68$, $\epsilon_{MCP} = 0.3492$), there is only a second order phase transition. For $n_{MTP} < n < n_{MCP}$ ($n_{MTP} \simeq 0.563$, $\epsilon_{MTP} = 0.36032$) there is a second order phase transition and a first order phase transition. For $1/2 \leq n < n_{MTP}$, there is only a first order phase transition. For $n_* < n < n_{MTP}$ ($n_* \simeq 0.54$, $\epsilon = 0.3508$), the metastable branch presents a second order phase transition.

6 The physical caloric curve

We have explained previously that the proper thermodynamical caloric curve to consider when we study phase transitions and ensembles inequivalence is the curve $T(E)$ where $T = 1/\beta$ is the thermodynamical temperature with $\beta = (\partial S/\partial E)_M$. However, in practice, the caloric curve that is experimentally or numerically accessible is the curve $\langle T_{kin}\rangle(E)$ that gives the averaged kinetic temperature as a function of the energy E. This is the one, for example, that is represented in Fig. 4 of Antoni & Ruffo [8]. It is therefore useful to study this curve specifically. We will call it the physical caloric curve. In dimensionless form, it is given by $\Theta(\epsilon)$. Several caloric curves $1/\Theta(\epsilon)$ have been plotted in Fig. 6 for different indices $n \geq 1/2$.

In order to understand their behavior, let us consider the asymptotic limit $x \to 0$.

From expressions (128) and (129), we can draw the following conclusions. Let us introduce the critical indices

$$\gamma_0 = \frac{1+\sqrt{17}}{4} \simeq 1.2807764... \quad (144)$$

$$n_0 = \frac{4}{\sqrt{17}-3} \simeq 3.5615528... \quad (145)$$

Let us first consider the case $n \geq 1/2$ so that $1 \leq \gamma \leq 3$. The quantity $2\gamma^2 - 5\gamma - 2$ is positive for $\gamma_* < \gamma < 3$, i.e. $1/2 \leq n < n_*$, showing that the energy increases as x increases. The quantity $2\gamma^2 - 5\gamma - 2$ is negative for $1 \leq \gamma < \gamma_*$, i.e. $n > n_*$, showing that the energy decreases as x increases. On the other hand, the quantity $2\gamma^2 - \gamma - 2$ is positive for $\gamma_0 < \gamma \leq 3$, i.e. $1/2 \leq n < n_0$, showing that the inverse kinetic temperature decreases as x increases. The quantity $2\gamma^2 - \gamma - 2$ is negative for $1 \leq \gamma < \gamma_0$, i.e. $n > n_0$, showing that the inverse kinetic temperature increases as x increases. This explains the behavior of the physical caloric curve $1/\Theta(\epsilon)$ close to the bifurcation point. Close to that point, we have

$$\Theta - \Theta_c = \frac{2\gamma^2 - \gamma - 2}{2\gamma^2 - 5\gamma - 2}(\epsilon - \epsilon_c) + ... \quad (146)$$

The physical specific heat is

$$C_{kin} = \frac{dE}{d\langle T_{kin}\rangle} = \frac{M}{2}\frac{d\epsilon}{d\Theta}. \quad (147)$$

At the bifurcation point, we have

$$C_{kin} = \frac{M}{2}\frac{2\gamma^2 - 5\gamma - 2}{2\gamma^2 - \gamma - 2}. \quad (148)$$

The physical specific heat close to the bifurcation point is positive for $1/2 \leq n < n_*$, negative for $n_* < n < n_0$ and positive again for $n > n_0$. It vanishes for $n = n_*$ and is infinite for $n = n_0$. Let us now consider the case $n < -1$ so that $0 < \gamma \leq 1$. In that case, the term $2\gamma^2 - \gamma - 2$ is always negative so that $1/\Theta$ increases as x increases. On the other hand, the term $2\gamma^2 - 5\gamma - 2$ is always negative so that ϵ decreases as x increases. Therefore, the physical specific heat is always positive.

Remark: We must be careful that we cannot deduce any stability result from this curve. For example, the Poincaré theorem [59,60] and the general results on ensembles inequivalence [50] apply to the thermodynamical caloric curve $T(E)$, not to the physical caloric curve $\langle T_{kin}\rangle(E)$. Furthermore, the notion of canonical ensemble is only defined in terms of the variables (E, T) via the Legendre transform $F = E - TS$, not in terms of the variables $(E, \langle T_{kin}\rangle)$. Note, in particular, that for $1 < n < n_0$, the solutions close to the bifurcation point have negative physical specific heat $C_{kin} = dE/d\langle T_{kin}\rangle$ although they are stable both in canonical and microcanonical ensembles (they have positive specific heat $C = dE/dT$)[22].

[22] A similar result has been observed recently for the Lynden-Bell distribution (in preparation).

7 The critical index $n_c = 1$

7.1 Analytical expressions

We have seen that the index $n_c = 1$ (i.e. $\gamma_c = 2$, $q_c = 3$) is particular because it corresponds to a canonical tricritical point. Furthermore, we will see that for this particular index, the algebra greatly simplifies and analytical results can be obtained. This is because the relationship (65) between the density and the potential is linear[23]. For $n_c = 1$, the density profile is

$$\rho(\theta) = A\left(1 + \frac{x}{2}\cos\theta\right)_+. \quad (149)$$

For $x < x_c = 2$, the deformed Bessel functions take the simple form

$$I_{2,0}(x) = 1, \qquad I_{2,1}(x) = \frac{x}{4}. \quad (150)$$

Then, we get

$$A = \frac{M}{2\pi}, \quad \eta = \eta_c = 2, \quad b = \frac{x}{4}, \quad (151)$$

$$\epsilon = \frac{1}{2} - \frac{x^2}{16}, \quad \Theta = \frac{1}{2} + \frac{x^2}{16}. \quad (152)$$

We note in particular that the polytropic temperature is constant $\eta = \eta_c = 2$ (i.e. $K_c = k/4$ in dimensional form) so that there exists an infinity of solutions (the range of magnetizations $-1/2 \leq b \leq 1/2$) with the same temperature. However, they have different energies (see Fig. 4) ranging from $1/4$ to $1/2$. We will show analytically in Sec. 8 that these solutions are stable in the microcanonical ensemble while they are degenerate in the canonical ensemble. In the range $1/4 \leq \epsilon \leq 1/2$, the thermodynamical caloric curve $\eta = \eta_c$ has an infinite specific heat $C = dE/dT = \infty$. The corresponding physical caloric curve is given by

$$\Theta = 1 - \epsilon. \quad (153)$$

It has a constant negative specific heat

$$C_{kin} = \frac{M}{2}\frac{d\epsilon}{d\Theta} = -\frac{M}{2}. \quad (154)$$

[23] Note that a similar linear relationship occurs in 2D turbulence between the vorticity and the stream function for minimum enstrophy states. Now, the enstrophy $\Gamma_2 = \int \omega^2\, d\mathbf{r}$, which is a quadratic functional, can be interpreted as a particular Tsallis functional with $q = 2$ (in our notations). This precisely corresponds to the case $\gamma = 2$ considered here (in 2D turbulence, we directly work in physical space so that q plays the role of γ). We may note that an approximate linear $\omega - \psi$ relationship has been observed in a plasma experiment [28,29] and interpreted as a case of incomplete violent relaxation [30]. It is interesting to note that the same index $\gamma = 2$ arises in the HMF model (see Sec. 7.2). Note, however, that in many other situations of 2D turbulence, the $\omega - \psi$ relationship is not linear, so that this relation is not universal and may lead to physical inconsistencies [30].

This is an example where the thermodynamical caloric curve and the physical caloric curve give very different results.

For $x > x_c = 2$, we have $\cos\theta_c = -2/x$ and the deformed Bessel functions take the form

$$I_{2,0}(x) = \frac{1}{2\pi}\left[\sqrt{x^2-4} + 2\arccos\left(-\frac{2}{x}\right)\right], \qquad (155)$$

$$I_{2,1}(x) = \frac{1}{2\pi}\left[\frac{1}{x}\sqrt{x^2-4} + \frac{x}{2}\arccos\left(-\frac{2}{x}\right)\right]. \qquad (156)$$

Then, we obtain

$$A = \frac{M}{\sqrt{x^2-4} + 2\arccos\left(-\frac{2}{x}\right)}, \quad \eta = \frac{x}{2I_{2,1}(x)}, \qquad (157)$$

$$b = \frac{I_{2,1}(x)}{I_{2,0}(x)}, \quad \epsilon = -\frac{I_{2,1}(x)^2}{I_{2,0}(x)^2} + \frac{2}{x}\frac{I_{2,1}(x)}{I_{2,0}(x)}, \qquad (158)$$

$$\Theta = \frac{I_{2,1}(x)^2}{I_{2,0}(x)^2} + \frac{2}{x}\frac{I_{2,1}(x)}{I_{2,0}(x)}. \qquad (159)$$

For $x \to +\infty$, we have the equivalents $I_{2,0}(x) \sim \frac{x}{2\pi}$ and $I_{2,1}(x) \sim \frac{x}{8}$. Therefore, the normalization constant behaves like $A \sim \frac{M}{x}$ and the density tends to the limit distribution

$$\rho(\theta) = \frac{M}{2}\cos\theta, \qquad (160)$$

for $\theta \leq \pi/2$. On the other hand, the thermodynamical parameters tend to

$$\eta \to 4, \quad b \to \frac{\pi}{4}, \quad \epsilon \to -\frac{\pi^2}{16}, \quad \Theta \to \frac{\pi^2}{16}. \qquad (161)$$

7.2 Application to the case $M_0 = 1$

We shall now apply our theory of polytropes to interpret the physical caloric curve shown in Fig. 4 of Antoni & Ruffo [8]. It is obtained from an initial waterbag distribution with magnetization $M_0 = 1$ and it has been confirmed by other groups [13,14]. Up to date, there is no explanation of the "anomalies" that take place close to the critical energy $U_c = 3/4$. These anomalies are: (i) the bifurcation from the homogeneous branch to the inhomogeneous branch takes place at a lower value of the energy, and (ii) the physical caloric curve presents a region of negative specific heat $U'(T) < 0$. It was noted in [18,26] that these anomalies cannot be explained in terms of Lynden-Bell's theory so that other approaches could be considered... We here argue that these anomalies can be explained naturally by assuming that the QSSs in that region are polytropic distributions with an index close to the critical one $n_c = 1$ (i.e. $\gamma_c = 2$ or $q_c = 3$).

We make the link between the notations of Antoni & Ruffo [8] and our notations [9] by setting $U = \epsilon/4 + 1/2$ and $T = \Theta/2$, where U is the energy and T the kinetic temperature. This amounts to taking $k = 2\pi/N$ and $M = N$ in the previous formulae and adding a constant in the energy (ground state). For $n = 1$, we find that the transition from the homogeneous states to the inhomogeneous states takes place for $\epsilon_c = 1/2$, i.e. $U_c = 5/8 \simeq 0.625$. On the other hand, for indices $n_* < n < n_0$, the physical specific heat $U'(T)$ is negative. In particular, for $n = 1$, we have $C_{kin} = \frac{dU}{dT} = \frac{1}{2}\frac{d\epsilon}{d\Theta} = -\frac{1}{2}$. This is at variance with Lynden-Bell's prediction. Note, however, that the branch of inhomogeneous polytropes exists only above the minimum energy $\epsilon = -\pi^2/16$, i.e. above $U = -\pi^2/64 + 1/2 \simeq 0.345$ (corresponding to $T \to \pi^2/32 \simeq 0.308$). Below this energy, we expect that the system reaches the Lynden-Bell distribution. The numerical caloric curve shows a good agreement with the Lynden-Bell prediction (equivalent to Boltzmann) in that region. However, this agreement should be ascertained by explicitly computing the distribution functions. Similarly, it should be checked whether the homogeneous states correspond to Lynden-Bell distributions (equivalent to Boltzmann distributions), polytropic distributions or something else.

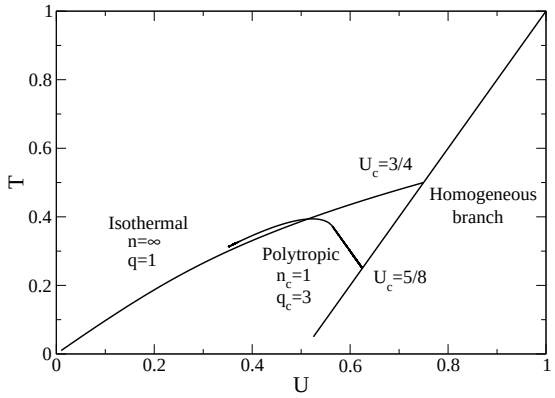

Fig. 21. Kinetic temperature T as a function of the energy U for $n = 1$. Our theory of polytropes seems to explain the anomalies displayed on the numerical caloric curve of Antoni & Ruffo [8] close to the critical energy, unlike the Lynden-Bell approach which leads to isothermal distributions.

In conclusion, our theory of polytropes qualitatively explains the "anomalies" displayed by the caloric curve of Antoni & Ruffo [8]. As in previous works [18,26], we justify these polytropic distributions as a result of incomplete violent relaxation and lack of ergodicity (inefficient mixing). We stress, however, that polytropes are not universal attractors in case of non-ergodicity and that other distributions could emerge. However, it turns out that polytropes play a special role. We have not tried to compare in more detail the theory and the observations in order to determine the best value of q (it may not be exactly $q = 3$ but it happens to be close). This is left for a future study where we will also determine numerically the distribution functions to check whether they can be fitted by $q \simeq 3$ polytropes. The simulations of Campa *et al.* [34] go in that direction but, since there are differences with the simulations of Latora *et al.* [14], a detailed study must be performed. Nevertheless, our approach brings a plausible explanation of the numerical results of Antoni & Ruffo [8] in

terms of Tsallis distributions (polytropes). Furthermore, the apparently selected index $q_c = 3$ is not completely arbitrary. First, it leads to distributions with a compact support, which is consistent with the phenomenology of incomplete mixing. Secondly, it happens to coincide with (or be close to) the critical index that appears in the theory. It is interesting to note that this value was found numerically [34] before the theory showed that it has a special meaning. All these results have to be confirmed.

8 Stability analysis

In the previous sections, we have determined critical points of entropy (or free energy) and we have plotted the corresponding series of equilibria. For some indices, we have found multiple equilibria for the same value of E (or K) and, in case of competition, we have compared the equilibrium entropy (or the equilibrium free energy) of the different solutions in order to select the optimal one. However, a more precise analysis should determine whether the selected solutions really are entropy maxima (or free energy minima) by investigating the sign of the second order variations of S (or F). This is a more complicated problem that will be solved only partially in the following sections.

8.1 Variational principles: general theory

8.1.1 Microcanonical ensemble

Basically, we have to solve the maximization problem

$$\max_f \{S[f] \,|\, E[f] = E,\, M[f] = M\}, \qquad (162)$$

where $S[f]$ is the Tsallis functional (11). To solve this problem, we can proceed in two steps. *First step:* we first maximize S at fixed E, M *and* $\rho(\mathbf{r})$. Since the specification of $\rho(\mathbf{r})$ determines M and W, this is equivalent to maximizing S at fixed E_{kin} and $\rho(\mathbf{r})$. Writing the first variations as

$$\delta S - \beta \delta E_{kin} - \int \alpha(\mathbf{r}) \delta \left(\int f \, d\mathbf{v} \right) d\mathbf{r} = 0, \qquad (163)$$

we obtain

$$f(\mathbf{r}, \mathbf{v}) = \left[\mu(\mathbf{r}) - \frac{(q-1)\beta}{q} \frac{v^2}{2} \right]_+^{1/(q-1)}. \qquad (164)$$

This critical point is the global maximum of entropy with the previous constraints since $\delta^2 S = -\frac{q}{2} \int f^{q-2} (\delta f)^2 \, d\mathbf{r} d\mathbf{v} \leq 0$ (the constraints are linear in f so their second variations vanish). The function $\mu(\mathbf{r})$ is determined by the density $\rho = \int f \, d\mathbf{v}$. This leads to the expression (38). From this expression (38), we can compute the pressure $p = \frac{1}{d} \int f v^2 \, d\mathbf{v}$ and we obtain the polytropic equation of state (27). We can now express the energy and the entropy as a function of ρ and p and we obtain expressions (51) and (52). These expressions are valid here out-of-equilibrium. *Second step:* we now have to solve the variational problem

$$\max_\rho \{S[\rho] \,|\, E[\rho] = E |\, M[\rho] = M\}, \qquad (165)$$

where S, E and M are given by Eqs. (51), (52) and (15). *Conclusion:* the solution of (162) is given by Eq. (164) [or (38)] where ρ is the solution of (165). Therefore, we have reduced the study of the initial variational problem (162) for the distribution function $f(\mathbf{r}, \mathbf{v})$ to the study of a simpler variational problem (165) for the density $\rho(\mathbf{r})$. Note that the two problems (162) and (165) are equivalent in the sense that the distribution function $f(\mathbf{r}, \mathbf{v})$ is a maximum of $S[f]$ at fixed E and M iff the corresponding density profile $\rho(\mathbf{r})$ is a maximum of $S[\rho]$ at fixed E and M.

The variational problem (165) has been studied by Chavanis & Sire [46] in arbitrary dimension of space. The first variations return the relation (33). Then, this distribution is a local maximum of entropy at fixed mass and energy iff (see Appendix D of [46]):

$$\frac{\delta^2 S}{\beta} = -\frac{1}{2}\gamma \int p \frac{(\delta\rho)^2}{\rho^2} \, d\mathbf{r} - \frac{1}{2} \int \delta\rho \delta\Phi \, d\mathbf{r} - \frac{2n}{d(2n-d)} \frac{1}{\int p \, d\mathbf{r}} \left[\int \left(\Phi + \frac{d}{2}\gamma \frac{p}{\rho} \right) \delta\rho \, d\mathbf{r} \right]^2 \leq 0, \qquad (166)$$

for all perturbations $\delta\rho$ that do not change mass at first order (the conservation of the energy has been taken into account in obtaining Eq. (166)).

8.1.2 Canonical ensemble

In the canonical ensemble, we have to solve the minimization problem

$$\min_f \{F[f] \,|\, M[f] = M\}, \qquad (167)$$

where $F = E - TS$ and $T = 1/\beta$. To solve this problem, we can proceed in two steps. *First step:* we first minimize F at fixed M *and* $\rho(\mathbf{r})$. Since the specification of $\rho(\mathbf{r})$ determines M, this is equivalent to minimizing F at fixed $\rho(\mathbf{r})$. Writing the first variations as

$$\delta F + T \int \alpha(\mathbf{r}) \delta \left(\int f \, d\mathbf{v} \right) d\mathbf{r} = 0, \qquad (168)$$

we obtain

$$f(\mathbf{r}, \mathbf{v}) = \left[\mu(\mathbf{r}) - \frac{(q-1)\beta}{q} \frac{v^2}{2} \right]_+^{1/(q-1)}. \qquad (169)$$

This critical point is the global minimum of free energy with the previous constraint since $\delta^2 F = \frac{q}{2} T \int f^{q-2} (\delta f)^2 \, d\mathbf{r} d\mathbf{v} \geq 0$ (the constraint is linear in f so its second variations vanish). The function $\mu(\mathbf{r})$ is determined by the density $\rho = \int f \, d\mathbf{v}$. This leads to the expression (38). From this expression (38), we can compute

the pressure $p=\frac{1}{d}\int fv^2\,d\mathbf{v}$ and we obtain the polytropic equation of state (27). We can now express the free energy as a function of ρ and p and we obtain expression (53). These expressions are valid here out-of-equilibrium. *Second step:* we now have to solve the variational problem

$$\min_{\rho}\{F[\rho]\,|\,M[\rho]=M\}, \tag{170}$$

where F and M are given by Eqs. (53) and (15). *Conclusion:* the solution of (167) is given by Eq. (169) [or (38)] where ρ is the solution of (170). Therefore, we have reduced the study of the initial variational problem (167) for the distribution function $f(\mathbf{r},\mathbf{v})$ to the study of a simpler variational problem (170) for the density $\rho(\mathbf{r})$. Note that the two problems (167) and (170) are equivalent in the sense that the distribution function $f(\mathbf{r},\mathbf{v})$ is a minimum of $F[f]$ at fixed M iff the corresponding density profile $\rho(\mathbf{r})$ is a minimum of $F[\rho]$ at fixed M.

The variational problem (167) has been studied by Chavanis & Sire [46] in arbitrary dimensions of space. The first variations immediately return the relation (33). Then, this distribution is a local minimum of free energy at fixed mass iff

$$\delta^2F=\frac{1}{2}\gamma\int p\frac{(\delta\rho)^2}{\rho^2}\,d\mathbf{r}+\frac{1}{2}\int\delta\rho\delta\Phi\,d\mathbf{r}\geq 0 \tag{171}$$

for all perturbations $\delta\rho$ that do not change mass at first order.

Remark 1: from the stability criteria (166) and (171), we clearly see that canonical stability implies microcanonical stability (but not the converse). Indeed, since the last term in Eq. (166) is negative, it is clear that if inequality (171) is satisfied, then inequality (166) is automatically satisfied. In general, this is not reciprocal and we may have ensembles inequivalence. However, if we consider a spatially homogeneous system for which Φ is uniform, the last term in Eq. (166) vanishes (since the mass is conserved) and the stability criteria (166) and (171) coincide. Therefore, for spatially homogeneous systems, we have ensembles equivalence.

Remark 2: the approach developed previously in the canonical ensemble can be generalized to any functional of the form (3) [49]. The minimization problem (167) is equivalent to (170) with the free energy $F[\rho]$ given by

$$F=\frac{1}{2}\int\rho\Phi\,d\mathbf{r}+\int\rho\int^{\rho}\frac{p(\rho')}{\rho'^2}\,d\rho'd\mathbf{r}, \tag{172}$$

where $p(\rho)$ is the equation of state associated to $C(f)$. A critical point of (172) satisfies the condition of hydrostatic balance

$$\nabla p=-\rho\nabla\Phi. \tag{173}$$

Then, this critical point is a local minimum of free energy at fixed mass iff

$$\delta^2F=\int\frac{p'(\rho)}{2\rho}(\delta\rho)^2\,d\mathbf{r}+\frac{1}{2}\int\delta\rho\delta\Phi\,d\mathbf{r}\geq 0 \tag{174}$$

for all perturbations $\delta\rho$ that do not change mass at first order. For the polytropic equation of state (27), this returns the previous results.

8.2 Application to the HMF model

Let us now apply the preceding results to the HMF model. We start by the canonical ensemble which is simpler in a first step.

8.2.1 Canonical ensemble

According to the results of Sec. 8.1.2, we have to solve

$$\min_{\rho}\{F[\rho]\,|\,M[\rho]=M\}, \tag{175}$$

with

$$F[\rho]=-\frac{\pi B^2}{k}+\frac{K}{\gamma-1}\int\rho^{\gamma}\,d\theta. \tag{176}$$

To solve this problem, we can again proceed in two steps. We first minimize $F[\rho]$ at fixed M *and* B. This gives

$$\rho_1(\theta)=A\left[1+\frac{\gamma-1}{\gamma}\lambda\cos\theta\right]_+^{\frac{1}{\gamma-1}}, \tag{177}$$

where the Lagrange multipliers A and λ are determined by the constraints M and B through

$$A=\frac{M}{2\pi I_{\gamma,0}(\lambda)}, \tag{178}$$

and

$$\frac{2\pi B}{kM}=\frac{I_{\gamma,1}(\lambda)}{I_{\gamma,0}(\lambda)}. \tag{179}$$

This is the global minimum of F with the previous constraints since $\delta^2F\geq 0$ (this can be deduced from Eq. (171) by taking $\delta\Phi=0$ since B is fixed). Then, we can express the free energy F as a function of B by writing $F(B)\equiv F[\rho_1]$. This gives

$$F(B)=-\frac{\pi B^2}{k}+\frac{K}{\gamma-1}\frac{M^{\gamma}}{[2\pi I_{\gamma,0}(\lambda)]^{\gamma-1}}\times\left(1+\frac{\gamma-1}{\gamma}\lambda\frac{2\pi B}{kM}\right)_+, \tag{180}$$

where λ is related to B by Eq. (179). Finally, (175) is equivalent to

$$\min_{B}\{F(B)\}, \tag{181}$$

in the sense that the solution of (175) is given by Eqs. (177)-(179) where B is the solution of (181). For given K and M (canonical ensemble), we just have to determine the minimum of a *function* $F(B)$ of the magnetization B. The critical points $F'(B)=0$ should return the condition (84) of equilibrium. Furthermore, the minima correspond to $F''(B)>0$. For isothermal distributions, the equations take a simple form and we can show [66] through simple graphical constructions (by studying the slopes of simple curves) that they return the well-known stability results. For polytropic distributions, it seems more difficult to study (181) at a general level.

Note that in terms of λ, related to the magnetization by (179), the normalized free energy (180) can be written

$$f(\lambda)=-\left[\frac{I_{\gamma,1}(\lambda)}{I_{\gamma,0}(\lambda)}\right]^2+\frac{1}{\gamma-1}\frac{1}{\eta}\frac{1}{I_{\gamma,0}(\lambda)^{\gamma-1}} \times\left[1+\frac{\gamma-1}{\gamma}\lambda\frac{I_{\gamma,1}(\lambda)}{I_{\gamma,0}(\lambda)}\right]_+. \quad (182)$$

Therefore, for each value of the polytropic temperature η, it suffices to study this function and determine its minima. Of course, this can be done easily for each η but it seems difficult to find a general criterion of stability. It seems even difficult to check (in the non-isothermal case) that $f'(\lambda)=0$ leads to $\lambda=x$ where x is given by Eq. (84).

However, some analytical results can be obtained for the critical index $n=1$ ($\gamma=2$). In that case, using Eq. (150) for $\lambda\leq 2$, the expression (182) of the free energy becomes

$$f(\lambda)=-\frac{\lambda^2}{16}+\frac{1}{\eta}\left(1+\frac{\lambda^2}{8}\right). \quad (183)$$

Its derivative is

$$f'(\lambda)=-\frac{\lambda}{8}+\frac{\lambda}{4\eta}. \quad (184)$$

For $\eta\neq\eta_c=2$, the only critical point $f'(\lambda)=0$ is $\lambda=0$ (homogeneous phase). This is a minimum for $\eta<\eta_c$ ($f''(0)>0$) and a maximum for $\eta>\eta_c$ ($f''(0)<0$). If we now consider the critical temperature $\eta=\eta_c=2$, we get

$$f(\lambda)=\frac{1}{2}. \quad (185)$$

Therefore, the solutions $0\leq\lambda\leq 2$ have the same free energy and the inhomogeneous branch is degenerate.

8.2.2 Microcanonical ensemble

Let us now consider the microcanonical ensemble. According to the results of Sec. 8.1.1, we have to solve

$$\max_{\rho}\{S[\rho]\,|\,E[\rho]=E,\,M[\rho]=M\}, \quad (186)$$

with

$$S[\rho]=-\left(n-\frac{1}{2}\right)\beta\int p\,d\theta, \quad (187)$$

$$E[\rho]=\frac{1}{2}\int p\,d\theta-\frac{\pi B^2}{k}. \quad (188)$$

To solve this problem, we can again proceed in two steps. We first maximize $S[\rho]$ at fixed E, M *and* B. This gives the optimal distribution (177) as in the canonical ensemble. This is the global maximum of S with the previous constraints since $\delta^2 S\leq 0$ (this can be deduced from Eq. (166) by taking $\delta\Phi=0$ since B is fixed). Then, we can express the entropy S and the energy E as a function of B by writing $S\equiv S[\rho_1]$ and $E=E[\rho_1]$. This gives

$$E=\frac{KM^\gamma}{2[2\pi I_{\gamma,0}(\lambda)]^{\gamma-1}}\left(1+\frac{\gamma-1}{\gamma}\lambda\frac{2\pi B}{kM}\right)_+-\frac{\pi B^2}{k}, \quad (189)$$

and

$$S=-\frac{2n-1}{C_n}\frac{1}{K^{\frac{2n}{2n-1}}}\left(E+\frac{\pi B^2}{k}\right), \quad (190)$$

where λ is related to B by Eq. (179). The first equation determines K as a function of B, E and M. Then, S becomes a function of B, E and M. Finally, (186) is equivalent to

$$\max_{B}\{S(B)\}, \quad (191)$$

in the sense that the solution of (186) is given by Eqs. (177)-(179) where B is the solution of (191). For given E and M, we just have to determine the maximum of a *function* $S(B)$ of the magnetization B. The critical points $S'(B)=0$ should return the condition (100) of equilibrium. Furthermore, the maxima correspond to $S''(B)<0$. Unfortunately, it seems difficult to study the maximization problem (191) at a general level, except in the isothermal case $\gamma=1$ [66].

Note that in terms of λ, related to the magnetization by (179), the normalized entropy can be written

$$s(\lambda)=-\left(n-\frac{1}{2}\right)\frac{\left(1+\frac{\gamma-1}{\gamma}\lambda\frac{I_{\gamma,1}(\lambda)}{I_{\gamma,0}(\lambda)}\right)_+^{\frac{2n}{2n-1}}}{(\epsilon+2\frac{I_{\gamma,1}(\lambda)^2}{I_{\gamma,0}(\lambda)^2})^{\frac{1}{2n-1}}I_{\gamma,0}(\lambda)^{\frac{2}{2n-1}}}. \quad (192)$$

Therefore, for each value of the energy ϵ it suffices to study this function and determine its maxima. Of course, this can be done easily for each ϵ but it seems difficult to find a general criterion of stability. It seems even difficult to check (in the non-isothermal case) that $s'(\lambda)=0$ leads to $\lambda=x$ where x is given by Eq. (100).

However, some analytical results can be obtained for the critical index $n=1$ ($\gamma=2$). In that case, using Eq. (150) for $\lambda\leq 2$, the expression (192) of the entropy becomes

$$s(\lambda)=-\frac{1}{2}\frac{\left(1+\frac{\lambda^2}{8}\right)^2}{\epsilon+\frac{\lambda^2}{8}}. \quad (193)$$

We easily obtain

$$s'(\lambda)=-\frac{\lambda\left(1+\frac{\lambda^2}{8}\right)\left(2\epsilon-1+\frac{\lambda^2}{8}\right)}{8\left(\epsilon+\frac{\lambda^2}{8}\right)^2}. \quad (194)$$

The critical points $s'(\lambda)=0$ are $\lambda=0$, corresponding to the homogeneous state, and $\lambda^2=x^2=8(1-2\epsilon)$, corresponding to the inhomogeneous solutions (152). Then, we find that

$$s''(x)=-\frac{1-2\epsilon}{2(1-\epsilon)}. \quad (195)$$

For $x \leq x_c = 2$, ϵ goes from 1/4 to 1/2. For these values, $s''(x) < 0$ implying that the inhomogeneous solutions $\lambda = x$ are entropy maxima (stable). On the other hand, for $\lambda = 0$, we have

$$s''(0) = \frac{1-2\epsilon}{8\epsilon^2}. \quad (196)$$

For $1/4 \leq \epsilon \leq 1/2$, we find $s''(0) > 0$ implying that the homogeneous solution $\lambda = 0$ is an entropy minimum (unstable).

9 Conclusion

The nature of quasi stationary states (QSS) in Hamiltonian systems with long-range interactions has created a lively debate in the statistical mechanics community [67]. Some researchers have argued that these QSSs could not be explained in terms of ordinary statistical mechanics and that it was necessary to use a new thermodynamics (Tsallis generalized thermodynamics) [68,3]. Other researchers have argued, on the contrary, that Tsallis thermodynamics was unsuccessful to explain QSSs [24,2]. This led to a violent polemic. We have since the start adopted an intermediate position [16,25,18,26,37]. In principle, the QSSs can be explained in terms of Lynden-Bell's theory, i.e. ordinary thermodynamics adapted to the Vlasov equation. However, this approach, as usual, *assumes ergodicity and efficient mixing*. There are cases where the system mixes well so that Lynden-Bell's prediction works well [19]. However, there are known situations were mixing is not efficient enough so that other distributions emerge [14,34]. This is always the case in astrophysics (Lynden-Bell's theory fails to describe galaxies) and in some situations of 2D turbulence [28-30][24]. Since there is no rigorous theory of non-ergodic (partially mixed) systems, we are open to new suggestions including the one by Tsallis.

The idea of Tsallis generalized thermodynamics, as we understand it, is to account for non ergodicity and incomplete mixing. It is based on the postulate that, in case of incomplete mixing, the system still maximizes an entropy but this is not the Lynden-Bell entropy. The Lynden-Bell entropy is obtained from a combinatorial analysis assuming that all microstates are equiprobable. This is the main postulate of statistical mechanics. Tsallis generalized thermodynamics rejects this equiprobability postulate and argues that complex systems "prefer" some regions of phase space rather than others. Then, Tsallis form of entropy is introduced as a postulate or justified from an axiomatic basis. We think that some works remains to be done in this area to determine to which situations of incomplete mixing Tsallis thermodynamics applies. Tsallis entropy certainly does not describe all types of incomplete mixing (e.g. galaxies are not stellar polytropes) but it may describe some of them. Therefore, Tsallis distributions (polytropes) are not universal attractors, but they are not useless neither. The results of this paper, and those reported in [34,37], suggest that Tsallis distributions can be useful to describe QSSs in some situations where the Lynden-Bell theory fails. This happens precisely in the anomalous region discovered long ago by Antoni & Ruffo [8], which stimulated all the activity on the HMF model. Therefore, our findings tend to show that the approaches of ordinary thermodynamics (Lynden-Bell) and generalized thermodynamics (Tsallis) are complementary rather than antagonistic (this is often the final outcome of a conflicting situation) [18].

We can also avoid entering in the polemic by taking the following simple position [47,39,25,49]. We can argue that, in case of incomplete violent relaxation, the system reaches a QSS that is a steady solution of the Vlasov equation on the coarse-grained scale. This QSS differs from the Lynden-Bell prediction but it is not possible to predict it as it depends strongly on the dynamics. Of course, we must select only nonlinearly dynamically stable steady states and this leads to investigate the variational problems of the form (4)-(5). These variational problems are *similar* to thermodynamical variational problems[25] but they lead to dynamical stability criteria, not thermodynamical stability criteria. This dynamical approach does not attempt to explain *how* the QSSs are selected. It just provides formal dynamical stability criteria for a large class of distribution functions. In that dynamical approach, polytropic distributions just appear as *particular steady states of the Vlasov equation* [47]. By contrast, the thermodynamical approach of Lynden-Bell, or its generalization [15], seeks to explain *how* the QSSs are selected and *predict* them from general (yet possibly arguable) considerations. We think that dynamics and thermodynamics are intermingled [47,49] and that much work remains to be done in this area. Also, the methods of chaos can be very useful to explain incomplete relaxation and lack of ergodicity [69,70]. The subject is certainly not closed.

A The condition of hydrostatic equilibrium

For any distribution function of the form $f = f(\epsilon)$ where $\epsilon = v^2/2 + \Phi(\mathbf{r})$ is the individual energy, using Eq. (21), one has

$$\nabla p = \frac{1}{d}\nabla\Phi \int f'(\epsilon) v^2 \, d\mathbf{v} = \frac{1}{d}\nabla\Phi \int \left(\frac{\partial f}{\partial \mathbf{v}}\cdot \mathbf{v}\right) d\mathbf{v}$$
$$= -\frac{1}{d}\nabla\Phi \int f \nabla_{\mathbf{v}}\cdot \mathbf{v} \, d\mathbf{v} = -\nabla\Phi \int f \, d\mathbf{v} = -\rho\nabla\Phi, \quad (197)$$

which is the condition of hydrostatic equilibrium (22).

[24] In the plasma experiment, although Lynden-Bell's prediction fails to describe the details of the distribution, it provides however a *fair* first order prediction [30]. The success or failure of Lynden-Bell's prediction can be more or less severe depending on the initial conditions and it is not possible to draw a general conclusion (see the analogy with the meandering course of the Mississippi River in [27]).

[25] This is the "Canada-Dry" analogy: in these variational problems, S has the color of an entropy, but it is not an entropy!

B Derivation of the polytropic density and pressure laws

For $n > d/2$, the polytropic DF can we written

$$f = A(\epsilon_m - \epsilon)_+^{n-d/2}. \quad (198)$$

The density and the pressure can be expressed as

$$\rho = AS_d Q_0(\Phi), \qquad p = \frac{1}{d} AS_d Q_2(\Phi), \quad (199)$$

with

$$Q_k = \int_0^{\sqrt{2(\epsilon_m-\Phi)}} \left(\epsilon_m - \Phi - \frac{v^2}{2}\right)^{n-d/2} v^{k+d-1} dv. \quad (200)$$

Setting $x = v^2/[2(\epsilon_m - \Phi)]$, we obtain

$$Q_k = 2^{(k+d-2)/2}(\epsilon_m - \Phi)^{n+k/2} \times \int_0^1 (1-x)^{n-d/2} x^{(k+d-2)/2} dx. \quad (201)$$

The integral can be expressed in terms of Gamma functions leading to

$$Q_k = 2^{(k+d-2)/2}(\epsilon_m - \Phi)^{n+k/2} \times \frac{\Gamma((d+k)/2)\Gamma(1-d/2+n)}{\Gamma(1+k/2+n)}. \quad (202)$$

Then, the density and the pressure can be expressed in terms of the potential Φ as in Eqs. (23)-(24).

For $n < -1$, the polytropic DF can we written

$$f = A(\epsilon_0 + \epsilon)^{n-d/2}. \quad (203)$$

The density and the pressure can be expressed as

$$\rho = AS_d R_0(\Phi), \qquad p = \frac{1}{d} AS_d R_2(\Phi), \quad (204)$$

with

$$R_k = \int_0^{+\infty} \left(\epsilon_0 + \Phi + \frac{v^2}{2}\right)^{n-d/2} v^{k+d-1} dv. \quad (205)$$

Setting $x = v^2/[2(\epsilon_0 + \Phi)]$, we obtain

$$R_k = 2^{(k+d-2)/2}(\epsilon_0 + \Phi)^{n+k/2} \times \int_0^{+\infty} (1+x)^{n-d/2} x^{(k+d-2)/2} dx. \quad (206)$$

The integral can be expressed in terms of Gamma functions leading to

$$R_k = 2^{(k+d-2)/2}(\epsilon_0 + \Phi)^{n+k/2} \times \frac{\Gamma((d+k)/2)\Gamma(-k/2-n)}{\Gamma(d/2-n)}. \quad (207)$$

Then, the density and the pressure can be expressed in terms of the potential Φ as in Eqs. (25)-(26).

C Derivation of the expression (51) of the entropy

In the expression (11) of the entropy, we have to evaluate $\int f^q \, d\mathbf{v}$. Let us first consider the case $q > 1$. Using Eq. (38) and defining $x = v^2/[2(n+1)K\rho^{1/n}]$, we get

$$\int f^q \, d\mathbf{v} = \frac{1}{Z^q} \rho^\gamma S_d 2^{\frac{d-2}{2}} [(n+1)K]^{d/2} \times \int_0^1 (1-x)^{n+1-\frac{d}{2}} x^{\frac{d-2}{2}} dx. \quad (208)$$

The integral can be evaluated in terms of Γ functions and we obtain

$$\int f^q \, d\mathbf{v} = \frac{1}{Z^q} \rho^\gamma S_d 2^{\frac{d-2}{2}} [(n+1)K]^{d/2} \times \frac{\Gamma(d/2)\Gamma(2-d/2+n)}{\Gamma(2+n)}. \quad (209)$$

Using the property $\Gamma(x+1) = x\Gamma(x)$ and the expression (39) of Z, the foregoing equation reduces to

$$\int f^q \, d\mathbf{v} = \frac{1}{Z^{q-1}} \rho^\gamma \frac{1-d/2+n}{1+n}. \quad (210)$$

Using the equation of state (27), we obtain

$$\int f^q \, d\mathbf{v} = \frac{1-d/2+n}{(n+1)KZ^{q-1}} p. \quad (211)$$

Combining Eqs. (39) and (28), it is easy to establish that

$$(n+1)KZ^{q-1} = \frac{1}{A^{q-1}}. \quad (212)$$

Substituting this identity in Eq. (211), we find that

$$\int f^q \, d\mathbf{v} = \left(1 - \frac{d}{2} + n\right) A^{q-1} p. \quad (213)$$

Recalling the definition of A after Eq. (19), we obtain

$$\int f^q \, d\mathbf{v} = \left(1 - \frac{d}{2} + n\right) \beta \frac{q-1}{q} p. \quad (214)$$

After simplification, this yields the simple result

$$\int f^q \, d\mathbf{v} = \beta p. \quad (215)$$

Substituting this identity in Eq. (11), we obtain Eq. (51). The case $q < 1$ can be treated similarly and yields the same final result.

References

1. *Dynamics and thermodynamics of systems with long range interactions*, edited by T. Dauxois *et al.*, Lecture Notes in Physics **602**, (Springer, 2002)

2. A. Campa, T. Dauxois, S. Ruffo, Physics Reports **480**, 57 (2009)
3. C. Tsallis, *Introduction to Nonextensive Statistical Mechanics*, (Springer 2009)
4. T. Konishi, K. Kaneko, J. Phys. A **25**, 6283 (1992)
5. S. Inagaki, T. Konishi, Publ. Astron. Soc. Japan **45**, 733 (1993)
6. S. Inagaki, Prog. Theor. Phys. **90**, 557 (1993)
7. C. Pichon, PhD thesis, Cambridge (1994)
8. M. Antoni, S. Ruffo, Phys. Rev. E **52**, 2361 (1995)
9. P.H. Chavanis, J. Vatteville, F. Bouchet, Eur. Phys. J. B **46**, 61 (2005)
10. J. Messer, H. Spohn, J. Stat. Phys. **29**, 561 (1982)
11. G. Battle, Commun. Math. Phys. **55**, 299 (1977)
12. J. Barré, F. Bouchet, T. Dauxois, S. Ruffo, J. Stat. Phys. **119**, 677 (2005)
13. V. Latora, A. Rapisarda, C. Tsallis, Phys. Rev. E **64**, 056134 (2001)
14. V. Latora, A. Rapisarda, C. Tsallis, Physica A **305**, 129 (2002)
15. C. Tsallis, J. Stat. Phys. **52**, 479 (1988)
16. P.H. Chavanis, *Statistical mechanics of two-dimensional vortices and stellar systems* in [1].
17. Y.Y. Yamaguchi, J. Barré, F. Bouchet, T. Dauxois, S. Ruffo, Physica A **337**, 36 (2004)
18. P.H. Chavanis, Eur. Phys. J. B **53**, 487 (2006)
19. A. Antoniazzi, D. Fanelli, J. Barré, P.H. Chavanis, T. Dauxois, S. Ruffo, Phys. Rev. E **75**, 011112 (2007)
20. D. Lynden-Bell, MNRAS **136**, 101 (1967)
21. A. Antoniazzi, D. Fanelli, S. Ruffo, Y. Yamaguchi, Phys. Rev. Lett. **99**, 040601 (2007)
22. P.H. Chavanis, G. De Ninno, D. Fanelli, S. Ruffo, in *Chaos, Complexity and Transport*, edited by C. Chandre, X. Leoncini and G. Zaslavsky (World Scientific, Singapore, 2008) p. 3
23. F. Staniscia, P.H. Chavanis, G. De Ninno, D. Fanelli, Phys. Rev. E **80**, 021138 (2009)
24. F. Bouchet, T. Dauxois, S. Ruffo, Europhysics News **37**,9 (2006)
25. P.H. Chavanis, Physica A **365**, 102 (2006)
26. P.H. Chavanis, Physica A **387**, 787 (2008)
27. J. Binney, S. Tremaine, *Galactic Dynamics* (Princeton Series in Astrophysics, 1987)
28. X.P. Huang, C.F. Driscoll, Phys. Rev. Lett. **72**, 2187 (1994)
29. B.M. Boghosian, Phys. Rev. E **53**, 4754 (1996)
30. H. Brands, P.H. Chavanis, R. Pasmanter, J. Sommeria, Phys. Fluids **11**, 3465 (1999)
31. R. Bachelard, C. Chandre, A. Ciani, D. Fanelli, Y.Y. Yamaguchi, Physics Letters A **373**, 4239 (2009)
32. A. Einstein, Annalen der Physik **33**, 1275 (1910)
33. E.G.D. Cohen, Physica A **305**, 19 (2002)
34. A. Campa, A. Giansanti, G. Morelli, Phys. Rev. E **76**, 041117 (2007)
35. P.H. Chavanis, A&A **401**, 15 (2003)
36. P.H. Chavanis, Eur. Phys. J. B **62**, 179 (2008)
37. A. Campa, P.H. Chavanis, A. Giansanti, G. Morelli, Phys. Rev. E **78**, 040102(R) (2008)
38. A. Taruya, M. Sakagami, Phys. Rev. Lett. **90**, 181101 (2003)
39. P.H. Chavanis, A&A **451**, 109 (2006)
40. A.S. Eddington, MNRAS **76**, 572 (1916)
41. H.C. Plummer, MNRAS **71**, 460 (1911)
42. A. Taruya, M. Sakagami, Physica A **307**, 185 (2002)
43. A. Taruya, M. Sakagami, Physica A **318**, 387 (2003)
44. A. Taruya, M. Sakagami, Physica A **322**, 285 (2003)
45. P.H. Chavanis, A&A **386**, 732 (2002)
46. P.H. Chavanis, C. Sire, Phys. Rev. E **69**, 016116 (2004)
47. P.H. Chavanis, C. Sire, Physica A **356**, 419 (2005)
48. P.H. Chavanis, L. Delfini, Eur. Phys. J. B **69**, 389 (2009)
49. P.H. Chavanis, AIP Conf. Proc. **970**, 39 (2008)
50. R. Ellis, K. Haven, B. Turkington, J. Stat. Phys. **101**, 999 (2000)
51. P.H. Chavanis, J. Sommeria, R. Robert, ApJ **471**, 385 (1996)
52. J. Jeans, MNRAS **76**, 70 (1915)
53. A.R. Plastino & A. Plastino, Physics Letters A **174**, 384 (1993)
54. J. Ipser, G. Horwitz, ApJ **232**, 863 (1979)
55. J. Ipser, ApJ **193**, 463 (1974)
56. R. Ellis, K. Haven, B. Turkington, Nonlinearity **15**, 239 (2002)
57. S. Tremaine, M. Hénon, D. Lynden-Bell, MNRAS **219**, 285 (1986)
58. S. Chandrasekhar *Principles of Stellar Dynamics* (University of Chicago Press, 1942)
59. J. Katz, MNRAS **183**, 765 (1978)
60. P.H. Chavanis, Int J. Mod. Phys. B **20**, 3113 (2006)
61. C. Sire, P.H. Chavanis, Phys. Rev. E **78**, 061111 (2008)
62. J. Barré, D. Mukamel, S. Ruffo, Phys. Rev. Lett. **87**, 030601 (2001)
63. P.H. Chavanis, Phys. Rev. E **65**, 056123 (2002)
64. T. Tatekawa, F. Bouchet, T. Dauxois, S. Ruffo Phys. Rev. E **71**, 056111 (2005)
65. P.H. Chavanis, L. Delfini, preprint
66. P.H. Chavanis, in preparation
67. *Dynamics and thermodynamics of systems with long range interactions: Theory and experiments*, edited by A. Campa *et al.*, AIP Conf. Proc. **970** (AIP, 2008).
68. A. Rapisarda, A. Pluchino, Europhysics News **36**, 202 (2005)
69. R. Bachelard, C. Chandre, D. Fanelli, X. Leoncini, S. Ruffo, Phys. Rev. Lett. **101**, 260603 (2008)
70. M.C. Firpo, Europhys. Lett. **88**, 30010 (2009)